Geoderma 463 (2025) 117573

Contents lists available at ScienceDirect

Geoderma

journal homepage: www.elsevier.com/locate/geoderma

Sensitivity of soil organic carbon stabilization indicators to 24 years of land-use change across soil depth

Eva Kanari [a,b,*], Kristiina Karhu [a,b], Anna-Reetta Salonen [c,d], Riitta Lemola [e], Helena Soinne [e], Pierre Barré [f], François Baudin [g], Kenichiro Mizohata [h], Markku Oinonen [i], Jenie Gil [j], Lukas Kohl [b,d,j], Taina Pennanen [e], Chao Liang [k], Jussi Heinonsalo [a,b]

[a] Department of Forest Sciences, University of Helsinki, Helsinki, Finland
[b] Institute for Atmospheric and Earth System Research / Forest Sciences, Faculty of Agriculture and Forestry, University of Helsinki, Helsinki, Finland
[c] Soil Biology Group, Department of Environmental Sciences, Wageningen University & Research, Wageningen, Netherlands
[d] Environmental Soil Science, Department of Agricultural Sciences, University of Helsinki, Helsinki, Finland
[e] Natural Resources Institute Finland (Luke), Helsinki, Finland
[f] Laboratoire de Géologie, École Normale Supérieure, CNRS, PSL University, IPSL, Paris, France
[g] Sorbonne Université, CNRS, ISTeP, Paris, France
[h] Department of Physics, University of Helsinki, Helsinki, Finland
[i] Finnish Museum of Natural History, University of Helsinki, Helsinki, Finland
[j] Department of Environmental and Biological Sciences, Faculty of Science, Forestry and Technology, University of Eastern Finland, Kuopio, Finland
[k] Institute of Applied Ecology, Chinese Academy of Sciences, Shenyang, China

ARTICLE INFO

Handling Editor: Dr Daniel Said-Pullicino

Keywords:
SOC dynamics
Agronomic experiment
Land management
Biogeochemical SOC pools
SOC fractionation

ABSTRACT

Soil organic carbon (SOC) and its dynamics are sensitive to changes in land management while assessments of SOC dynamics rely on different indicators of SOC stabilization and are often restricted to topsoil. Here, we evaluated six indicators of SOC stabilization along a 70 cm soil profile under long-term land-use change. Using an agronomic experiment including an unmanaged meadow and two cropland treatments, we quantified isotopic signatures (^{14}C and $\delta^{13}C$), size (mineral-associated OC; MaOC) and thermal (Rock-Eval® and PARTY$_{SOC}$-derived centennially stable C; C_S) fractions, and biochemical composition (amino sugar-derived microbial necromass C; MNC, and glomalin-related soil proteins; GRSP). Isotopic signatures and thermal analysis indicated older SOC (+~5000 years), a decreasing influence of fresh C (+0.7 ‰ $\delta^{13}C$) and higher proportion of C_S (by 75 %) with depth. In the cropland compared to the meadow, mean SOC age increased by ~ 250 years, $\delta^{13}C$ was enriched by 0.75 ‰ and C_S was 27 % higher. The proportion of MaOC reflected a slight increase in SOC stabilization with depth (6 %) but decreased in the cropland compared to the meadow (−5%). The proportions of the two biochemical indicators to total OC decreased with depth (−67 % for MNC and − 78 % for GRSP), following the same trend as bulk SOC, while the proportion of MNC decreased (−15 %) and GRSP increased but with very high uncertainties (37 ± 20 %) in the cropland compared to the meadow. Our results suggest that different indicators likely represent SOC stabilization at different scales, and their validity should be assessed across soil layers.

1. Introduction

Soil organic carbon (SOC), the largest terrestrial organic C reservoir (Friedlingstein et al., 2023), has a recognized major role for soil health and climate regulation (FAO & ITPS, 2015; FAO, 2017). One fourth of the global potential of nature-based solutions to mitigate climate change lies in managing SOC by protecting current stocks and maximizing potential sinks in degraded soils (Bossio et al., 2020). Depletion of SOC stocks can result from conversion of land under native vegetation to cropland, or after intensification of agriculture, especially when it involves high biomass exports (Heikkinen et al., 2013; Kopittke et al., 2022; Sanderman et al., 2017; Smith, 2008). Examples of practices with positive impact on SOC stocks are also known e.g., use of cover crops and improvement of soil quality after use of soil amendments (Kaspar and Singer, 2015; Pellerin et al., 2020; Sanderman et al., 2017). While the influence of land management on bulk topsoil OC is well documented

* Corresponding author at: Department of Forest Sciences, University of Helsinki, Helsinki, Finland.
E-mail address: eva.kanari@helsinki.fi (E. Kanari).

https://doi.org/10.1016/j.geoderma.2025.117573
Received 26 June 2025; Received in revised form 20 October 2025; Accepted 22 October 2025
Available online 3 November 2025

(Guo and Gifford, 2002; Huang et al., 2024; Li et al., 2018; Poeplau et al., 2011), studies focusing on SOC dynamics including entire depth profiles have only recently become more abundant (Ding et al., 2025; Hobley et al., 2017; Li et al., 2025; Poeplau and Don, 2013; Shi et al., 2020; Styc et al., 2025). Meanwhile, the impacts of land management vary above and below 30 cm (Emde et al., 2024; Tautges et al., 2019) and both the concentration and dynamics of SOC are strongly controlled by soil depth (Chirol et al., 2025; Hicks Pries et al., 2023; Lorenz and Lal, 2005).

The need to include subsoil when evaluating the C storage potential of soils and the response of current SOC stocks to environmental and climatic changes has been highlighted in recent years (Balesdent et al., 2018; Gross and Harrison, 2019; Guan et al., 2016; Hicks Pries et al., 2023; Hobley et al., 2017; Mathieu et al., 2015), as subsoil could have an important C storage potential in the long term. This is due to the combined effect of longer mean residence times, lower SOC concentrations observed in deeper soil layers that can be seen as a SOC deficit, and the important volume of the soil layer below 30 cm (Batjes, 1996; Jobbagy and Jackson, 2000). Still, the great variation in SOC residence times observed along soil profiles and in different locations (Elzein and Balesdent, 1995; Jenkinson and Coleman, 2008; Mathieu et al., 2015; Shi et al., 2020), makes SOC longevity a main concern considering climate change mitigation (Chenu et al., 2019; Stockmann et al., 2013) and a limiting uncertainty regarding SOC credits in carbon markets (Dynarski et al., 2020).

Multiple stabilization processes have been proposed for reducing the accessibility of SOC to the microbial decomposer community, with advances in their conceptualization in the last decades. Our understanding has evolved from the oversimplified idea of chemical recalcitrance of soil organic matter (SOM) due to its molecular structure, to a holistic view as an ecosystem property influenced by biotic (e.g., plant inputs, microbial community abundance and diversity) and abiotic factors (e.g., soil temperature, moisture, texture, and mineralogy; Marschner et al., 2008; Schmidt et al., 2011).

Based on the above-mentioned processes, a variety of empirical indicators focusing on the isotopic, physico-chemical and biochemical characteristics of potentially stabilized SOC have been developed. As for any other organic material, ^{14}C radioactive decay has been used to estimate the mean age of SOC up to millennial time scales and model its turnover time (Sierra et al., 2017; Torn et al., 2009, 1997; Trumbore et al., 1989). A second indicator based on the isotopic signature of SOC often used in studies of SOC dynamics on the multidecadal scale is the abundance of the ^{13}C stable isotope (Chen et al., 2005; Hobley et al., 2017; Hou et al., 2019). In sites without vegetation shifts between C3 and C4 plants, dynamics of $\delta^{13}C$ are influenced by changes in fresh organic matter inputs (as plant biomass tends to be ^{13}C-depleted compared to bulk SOC) and decay (associated to ^{13}C enrichment due to preferential lighter isotope utilization during microbial processing of SOC; Balesdent & Mariotti, 1996; Krüger et al., 2024).

One of the most widely used application-oriented SOC stabilization indicators is the mineral associated organic carbon (MaOC), which can be stabilized in soils mainly due to its close association with clay-sized minerals (Cambardella and Elliott, 1992; Cotrufo and Lavallee, 2022; Lavallee et al., 2020). Partly of microbial origin but also made up of dissolved organic carbon and breakdown products, its stabilization depends on physicochemical interactions with mineral surfaces, representing barriers to the decomposer community (Liang et al., 2017; Manzoni and Cotrufo, 2024). Its mean residence time in soils, assessed with the ^{14}C method, has been shown to vary from decades to centuries (Kleber et al., 2015; Lavallee et al., 2020), while studies using the $\delta^{13}C$ technique have shown that MaOC separated by size fractionation can have longer turnover times than the coarser particulate OC (POC; Balesdent, 1996).

Thermal analysis quantifies the energy required for thermal degradation (i.e., pyrolysis or oxidation) of organic compounds. It was proposed as a proxy for SOC stabilization after being empirically linked to *in situ* SOC biogeochemical persistence in long-term bare fallow experiments (Barré et al., 2016), mean SOC age according to the ^{14}C method (Plante et al., 2013) and biological SOC stability (Gregorich et al., 2015; Soucémarianadin et al., 2018). Based on Rock-Eval® thermal analysis results and samples from long-term experiments with observed SOC biogeochemical stability, a machine learning model, PARTY$_{SOC}$, was built, predicting the size of the centennially persistent SOC pool, here referred to as C_S (Cécillon et al., 2021; Cécillon et al., 2018).

Following the observation that in well aerated mineral soils a significant amount of SOC is microbially processed (Angst et al., 2021; Liang et al., 2017) and measurements confirming that microbial residues comprise a significant proportion of SOC (24–54 %; Wang et al., 2021), the concentration of amino sugars in soils was proposed as a biochemical indicator of SOC stabilization. As constituents of microbial necromass, amino sugars indicate the efficiency of the microbial community in turning plant-derived C into microbial residues, i.e., into compounds with a greater adsorption potential (Liang et al., 2017; Liang et al., 2019), that can be stabilized through association with soil minerals (Sokol et al., 2022). Moreover, the argument that older subsoil C is more intensively microbially processed supports the use of amino sugars as an indicator of stabilized SOC (Ahrens et al., 2015).

Another potential biochemical indicator for SOC stabilization is the concentration of glomalin-related soil proteins (GRSP). GRSP represents an operationally defined fraction of SOM that is extracted by autoclaving soil in a neutral or in an alkaline citrate solution (Wright and Upadhyaya, 1996). It was thought to originate from arbuscular mycorrhiza that in turn have been associated with the ability of soil to form aggregates, with a potential effect on carbon stabilization (Rillig, 2004). Even though the origin and composition of GRSP are under debate (Holátko et al., 2021; Staunton et al., 2020), its contribution to the stabilized SOC fraction is still considered relevant because of the high adsorption potential of proteins to mineral surfaces that can act as an important protection mechanism and because of its relative chemical recalcitrance compared to simpler amino acids (Carter et al., 2007; Kedi et al., 2013).

In this work we investigated the evolution of the above-mentioned SOC stabilization indicators (Fig. 1), along depth profiles (70 cm) of a 24-year long agronomic field experiment including two cropland treatments and an adjacent natural meadow (more details provided in section 2.1). The aims of the study were to assess the effect of land management

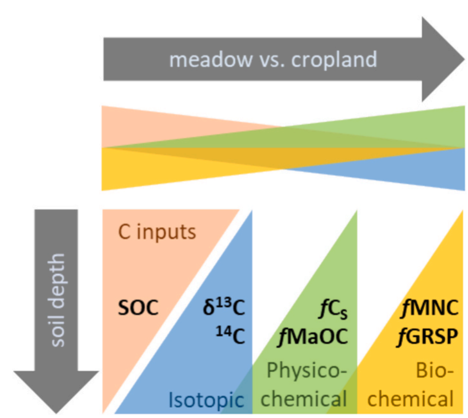

Fig. 1. Overview of the studied indicators of SOC stabilization. Triangles show their expected evolution with depth and in the cropland compared to the meadow. Soil organic carbon (SOC) in orange, isotopic indicators, mean SOC age derived by ^{14}C dating and $\delta^{13}C$ natural abundance, in blue, physico-chemical indicators, mineral associated fraction of SOC (fMaOC) and centennially stable SOC (fCs) according to thermal analysis, in green, and biochemical indicators, microbial necromass SOC (fMNC) derived from amino sugar analyses and glomalin-related soil proteins (fGRSP) as SOC weight percentage, in yellow. (For interpretation of the references to colour in this figure legend, the reader is referred to the web version of this article.)

on SOC dynamics along the soil profile and evaluate the relationships amongst indicators and between indicators and soil properties. As SOC in subsoil is more slowly cycling and less reactive to environmental changes than topsoil SOC, we hypothesized that (H1) the stabilization of SOC expressed by all indicators would vary with depth, with increasingly stable SOC proportion in the deep soil layers. After conversion of the grassland to cropland, a transition accompanied by a decrease in fresh C inputs, we expected (H2) the contribution of old/stabilized SOC to total SOC defined by isotopic and physico-chemical indicators to increase. (H3) In contrast, we expected the increased disturbance in the cropland compared to the meadow to have a decreasing effect on the relative proportions of the two microbial-derived biochemical indicators. As shown in previous studies and mentioned above, we expected (H4) clay content and the concentration of metal oxides to correlate with SOC stabilization. Finally, we discuss similarities and differences between the indicators with respect to the sizes of the different SOC pools, their evolution with depth and their reaction to land use change.

2. Materials and methods

2.1. Study site and soil sampling

The Yöni field experiment was established in Jokioinen, South-West Finland (60°51′44.5″N 23°31′24.5″E) between 1990 and 1995 by MTT Agrifood Research Finland and is maintained by the Natural Resources Institute Finland (Luke). A detailed description of the site and the cultivation history can be found in Salonen et al. (2023). The soil type was classified as a Vertic Stagnosol (IUSS Working Group WRB, 2015; Yli-Halla, 2000) and the whole field had a common land-use history before the onset of the experiment. Deforestation occurred in the beginning of the 20th century (Gylden, 1850, cited in Salonen et al., 2023), followed by multiple decades of use as a managed grassland (satellite image archive, 1956; Finnish land survey). The field was artificially drained in 1989 to a depth of 1 m.

At the establishment of the agronomic experiment, the field was split in 3 treatments: (i) an organic and (ii) a conventional cropping system, each with 6 plots in a randomized blocks design, and (iii) a part of the field was left to evolve as a natural meadow. The two cultivated systems were similar regarding plants in rotation (spring barley, perennial grasses, winter rye, oat, and pea), amount of residue returned to the soil, and ploughing depth (20 cm) and frequency. The organic system received cattle manure, whereas mineral fertilizer and herbicides were used in the conventional system. Salonen et al. (2023) summarize the average yearly nutrient inputs from fertilization to be 10 kg ha^{-1}P, 50 kg ha^{-1}N, 620–730 kg ha^{-1}C in the organic and 26 kg ha^{-1}P, 95 kg ha^{-1}N in the conventional system. No management operations (e.g., mowing, grazing, or exogenous C inputs) were conducted in the natural meadow other than removal of any emerging trees.

For this study, soil samples were taken from three replicate plots for each of the two cropland treatments; one soil core per replicate plot, collected in 2019. Soil cores from the adjacent meadow were also available in triplicate. As described by Salonen et al. (2023), the soil present in the cores was split in 10 cm increments from the surface down to 40 cm depth. In the remaining 40–70 cm section, changes in SOC concentration with depth were negligible and thus the remaining soil material in each core was mixed to a homogenized sample. The laboratory analyses described below were conducted on the available soil cores resulting in 3 replicates per soil layer per treatment, except for GRSP. GRSP and the data collected from the study by Salonen et al. (2023) i.e., SOC fractions (POC and MaOC) and soil characteristics were measured on three cores per plot resulting in 9 replicates per soil layer per treatment.

In addition, archived SOC concentration data were processed to illustrate the SOC concentration evolution at each treatment since the onset of the experiment (Supplementary material, Fig. S1).

2.2. Soil properties and SOC fractions

Basic soil properties including SOC content, pH, Al- and Fe-oxide concentrations, root biomass, soil bulk density and soil texture, were previously published in Salonen et al. (2023) and are provided in Table S1. SOC concentration was similar in the two cropping systems and higher in the meadow along the soil profile (Table S1; Fig. 2a). In all three treatments SOC concentration decreased with depth from 33, 35 and 70 g kg soil^{-1} in the top (0–10 cm) layer of the conventional, organic cropping system and meadow, respectively, to 3 g kg soil^{-1} in the deepest layer in all treatments. There was a statistically significant ($p = 0.0495$) higher SOC concentration in the meadow compared to the cropping systems in the four topmost layers (0–40 cm). We note that some differences in soil properties existed between the two land uses, with meadow having a constant clay content along the depth profile (700 g kg soil^{-1}), while cropland showed lower clay concentration in the topsoil (530 g kg soil^{-1}), increasing with depth, and reaching the same value as meadow in the deepest layer (Table S1). A similar trend was evident for the concentration of aluminum oxides and iron oxides (both higher in meadow than in cropland, with the concentration of Al-oxides converging and the concentration of Fe-oxides diverging in the subsoil). Meadow also had a slightly lower pH than the cropland below 30 cm and a slightly higher C/N ratio (Table S1). From the same publication we retrieved organic carbon present in the physical size fraction larger (POC) and finer than 53 μm (MaOC), fractionated according to the protocol by Cotrufo et al. (2019) with the exception that field moist soil was used instead of air dried (to avoid aggregation of heavy clay soil). We estimated that approximate yearly inputs in the meadow based on average national values and the method described in Palosuo et al. (2015), were 904 kg C ha^{-1} in total, 411 kg C ha^{-1} as aboveground and 493 kg C ha^{-1} as belowground deposition. Annual above- and belowground C inputs in the cropping systems were on average 176 kg C ha^{-1} and 186 kg C ha^{-1} in the organic and 182 kg C ha^{-1} and 263 kg C ha^{-1} in the conventional system. Accounting for manure additions reported in Salonen et al. (2023) brought the total C inputs to approximately 578 and 263 kg C ha^{-1} for the organic and conventional system, respectively. All reported values were corrected for humification using coefficients from Mattila et al. (2022).

2.3. Radiocarbon dating

Analysis of the radioactive ^{14}C isotope was conducted at the Laboratory of Chronology (Finnish Museum of Natural History, University of Helsinki), following the experimental protocol described in Uusitalo et al. (2022). Carbon was extracted from the soil sample through combustion in an Elemental Analyzer (Thermo Scientific Flash 2000 NC). Multiple combustions were performed in case of low C content to obtain ca. 1 mg C needed for AMS analyses. The CO_2 released was cryogenically captured, purified, and graphitized using zinc and iron catalysts (EA-HASE method; Palonen, 2015). The amount of radiocarbon present in the sample was measured using accelerator mass spectrometry (AMS, University of Helsinki) with an accuracy of < 0.2 % (Palonen and Tikkanen, 2015; Tikkanen et al., 2004). Radiocarbon age was given in radiocarbon years before 1950 (before present i.e. BP) and the associated uncertainty included statistical errors due to sample and reference measurement errors. The ^{14}C ages were normalized for isotopic fractionation to correspond to the value −25 ‰ using $\delta^{13}C$ measured by AMS. The given ages were converted to calendar years using the Intcal20 correction curve (Reimer et al., 2020) and Oxcal 4.4.4. software (Bronk Ramsey, 2009).

2.4. Isotopic signature $\delta^{13}C$

Analysis of natural abundance of the stable isotope ratio $^{13}C/^{12}C$ was conducted at the Stable Isotope Laboratory of the University of Eastern Finland. During sample preparation soils were dried at 60 °C for 48 h,

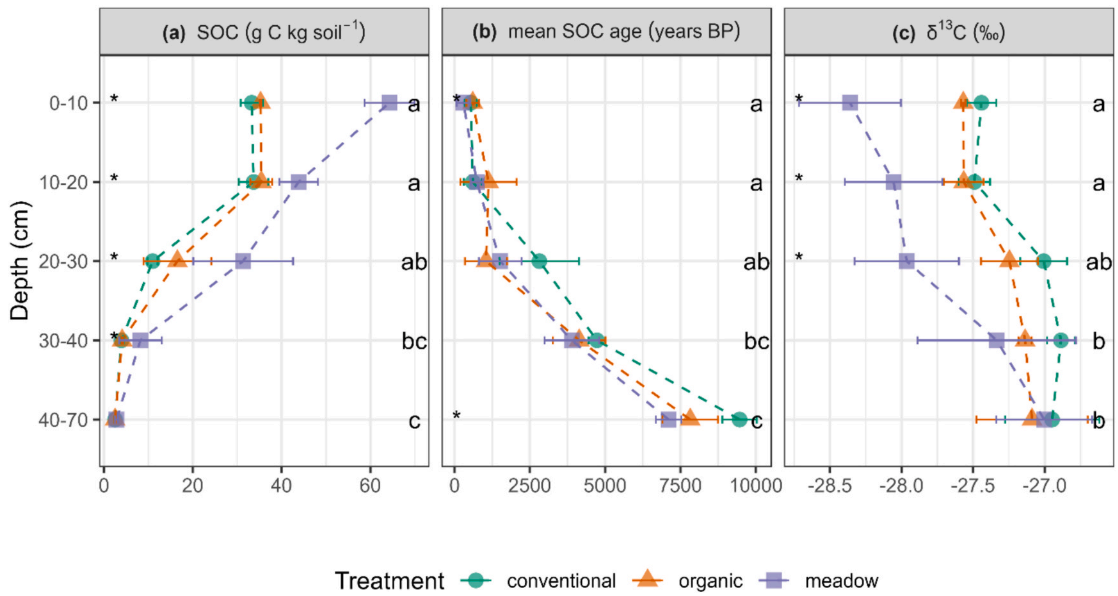

Fig. 2. a-c: Depth profiles of SOC concentration (data fromSalonen et al., 2023), SOC age and $\delta^{13}C$ at the three treatments of the Yöni field experiment. Points represent mean values and error bars show the standard deviation (n = 3). Stars indicate statistically significant differences between the two land uses in each layer (Kruskal Wallis test; p = 0.05). Significant changes with depth regardless of the treatment are indicated by different letters (Kruskal Wallis and Dunn's test for multiple comparisons; p-values adjusted with the Bonferroni method).

homogenized through ball-milling (250 µm) and weighed into tin capsules. Measurement of $\delta^{13}C$ of SOC was performed using an elemental analyzer coupled to an isotope ratio mass spectrometer (EA-IRMS), which included a Thermo Finnigan DELTA XP Plus IRMS, Flash EA 1112 Series Elemental Analyzer, and a Conflow III open split interface (Thermo Fisher Scientific, Bremen, Germany). During each analytical run two reference materials were measured: (a) USGS-40, an international reference material used for calibration of isotope values, and (b) wheat flour with certified $\delta^{13}C$ (IVA Analysetechnik; Meerbusch, Germany) used for correction of sample amount effects, and for quality control. All stable isotope ratios are reported in the delta notation ($\delta^{13}C$) relative to the V-PDB standard (Coplen, 2011). The reproducibility of 10 standard runs by EA-IRMS was typically better than 0.1 ‰ (1σ, n = 10). The long-term analytical precision of this analysis was ± 0.24 ‰ (1SD) and accuracy was 0.07 ‰.

2.5. *Rock-Eval® thermal analysis and the PARTY$_{SOC}$ machine-learning model*

Soil samples were analyzed using a Rock-Eval 6® Turbo apparatus (Vinci Technologies) at Institut des Sciences de la Terre (Sorbonne University). Approximately 60 mg of each finely ground (<250 µm) sample underwent pyrolysis under N_2 gas flow and thereafter oxidation under dried and CO_2-free ambient air. The heating cycle applied during pyrolysis started with a three-minute isotherm at 200 °C followed by a temperature increase of 30 °C min^{-1} to 650 °C (Barré et al., 2023). During oxidation a one-minute isotherm was applied at 300 °C, followed by a temperature increase of 20 °C min^{-1} to 850 °C, followed by a five-minute isotherm at 850 °C (Barré et al., 2023). The output of the analysis consisted of five thermograms describing the thermal decomposition of each sample, as detected by a flame ionization detector (HC pyrolysis) and an infrared cell (CO and CO_2, pyrolysis, and oxidation). Upper temperature integration limits for Rock-Eval® temperature parameters were set at 560 °C for the CO and CO_2 pyrolysis thermograms, and at 611 °C for the CO_2 oxidation thermograms (Cécillon et al., 2018). Based on the five thermograms and using the R scripts published by Cécillon (2021) available on the Zenodo platform 18 Rock-Eval® parameters were calculated and used as input for the European version of the PARTY$_{SOC}$ model (Cécillon et al., 2021). The model uses Rock-Eval® thermal analysis parameters as predictors to estimate the centennially stable SOC proportion (fC_S) in a soil sample according to a trained non-parametric random forest machine learning algorithm. In this study, the obtained fC_S of each sample was converted to centennially stable SOC content (C_S) through multiplication by the total SOC content of the same sample. According to this method, the remaining SOC is considered as centennially active (C_A). The European version of the model PARTY$_{SOC}$v2.0$_{EU}$ was used without any adaptation.

2.6. *Amino sugar analysis*

Soil samples were analyzed following the method developed by Zhang & Amelung (1996), described in detail in Meyer et al. (2023). The procedure involves breaking down of the microbial cell walls through acid hydrolysis (IS1 myo-inositol) followed by an evaporation step and pH-adjustment which allows metal ions and organic compounds to precipitate. This experimental protocol was designed to measure the concentration of four distinct amino sugars: glucosamine (GlcN), galactosamine (GalN), mannosamine (ManN), and muramic acid (MurN). Based on the concentration of MurN and using a conversion factor of 45 the necromass carbon of bacterial origin was calculated (Appuhn & Joergensen, 2006; Engelking et al., 2007; Equation (1). Fungal necromass carbon was calculated in line with Appuhn and Joergensen (2006) and Faust et al. (2017), using the molecular weight of GlcN and MurN, and the assumption that muramic acid and glucosamine occur at a 1:2M ratio in bacterial cells Equation (2). Finally, we calculated the total microbial necromass carbon (MNC) by adding the two fractions Equation (3).

$$\text{Bacterial necromass } C\left(mg\ C\ g\ soil^{-1}\right) = MurN\left(mg\ C\ g\ soil^{-1}\right) \bullet 45 \quad (1)$$

$$\text{Fungal necromass } C\left(mg\,C\,g\,soil^{-1}\right) = \left(GlucN\ \left(mg\,C\,g\,soil^{-1}\right)/179.19\ \left(g\,mol^{-1}\right) - 2 \bullet MurN\ \left(mg\,C\,g\,soil^{-1}\right)/251.23\left(g\,mol^{-1}\right)\right) \bullet 179.19\left(g\,mol^{-1}\right) \bullet 9 \quad (2)$$

$$\text{Microbial necromass } C\ \left(mg\ C\ g\ soil^{-1}\right) = \text{Bacterial necromas } C + \text{Fungal necromass } C \quad (3)$$

2.7. Glomalin-related soil proteins analysis

The GRSP fraction was extracted in triplicate from all soil samples (sieved at 200 μm) at the Viikki laboratory in the Natural Resources Institute Finland (Luke). GRSP was extracted by autoclaving 250 mg of soil in neutral sodium citrate solution (20 mM) at 121 °C for 30 min. After cooling at room temperature, the supernatant solution was separated by centrifugation at 15,000g for 10 min. A second centrifugation of the supernatant for another 5 min was conducted to ensure complete phase separation. The extract was diluted in microplates by combining 250 μL Bradford reagent (Bio-Rad Quick-Start™, Hercules, CA) with 20 μL aliquots of samples at various dilutions with sodium citrate (1:1, 2:3, 1:4). The mixtures were homogenized by shaking the microplates gently on a rotary shaker and thereafter removing air bubbles by short spinning at centrifuge. Absorbances were measured at 465 and 595 nm using a microplate reader (BMG Labtech, Multimode CLARIOstar). Sample and reagent blanks (diluted in 1 M HCl) were also measured at 465 nm and the values were subtracted before calculation of the soil protein content. The assay was calibrated using bovine serum albumin in the range 0–200 mg L − 1 and absorbance at 595 nm (Moragues-Saitua et al., 2019).

2.8. Data analysis

For comparing the effect of management practices on bulk SOC and on the stabilized SOC pools, the measured concentrations of SOC, MaOC, C_S, MNC and GRSP were converted to stocks according to the Equivalent Soil Mass (ESM) method (Ellert and Bettany, 1995; Lee et al., 2009; Wendt and Hauser, 2013), using the R script by Ferchaud et al. (2023). This was done to account for differences in soil bulk density, caused by compaction after conversion of the grassland to cropland, and thus erroneous comparisons of non-equivalent fixed sampled soil depths. To stay as close as possible to the initial soil layers we used the treatment with the lightest sampled soil cores, i.e., the average of three replicates for meadow, to define a reference cumulative soil mass to be reached in each layer. The following soil masses were used as the constant metric defining the five layers in all the soil cores: 0–717, 717–1790, 1790–3130, 3130–4580, and 4580–7500 t ha^{-1}, and they were reached at soil depths of 8 ± 2, 17 ± 3, 26 ± 3, 36 ± 3, 56 ± 3 cm.

We also summarized the difference in the ESM calculated stocks cumulatively for the topsoil (0–3000 t ha^{-1}; corresponding to 26 ± 3 cm soil depth), the whole soil profile (0–7500 t ha^{-1}; corresponding to 56 ± 3 cm soil depth) and the subsoil (calculated as the difference between the two). To visualize the difference in SOC and SOC stabilization parameters between the two land-uses, we calculated the relative change in their stocks as shown in Equation (4). We also calculated the relative change per cm soil depth by dividing each estimate by the corresponding soil layer thickness, similarly to Poeplau and Don (2013), to remove the influence of the different volumes of soil considered in each of the three soil profile sections.

$$\text{Relative } \Delta X\, stock(\%) = (X \text{ stock in cropland} - X \text{ stock in meadow})/X \text{ stock in meadow} \times 100 \quad (4)$$

where X represents the studied parameters SOC, MaOC, C_S, MNC and GRSP.

To evaluate changes in SOC stabilization with depth, we converted concentrations of SOC pools to proportions (indicated as *f*MaOC, *f*C_S and *f*MNC), by dividing the measured concentrations with the SOC content of each sample Equation (5). In the same manner, for GRSP we calculated a weight proportion of total SOC instead (*f*GRSP), to avoid possible errors due to the uncertainty associated with the C content of this operationally defined and isolated fraction.

$$fX(\%\ \textbf{or wt}.\%) = X\left(g\,C\,kg\,soil^{-1}\ \textbf{or g GRSP kg soil}^{-1}\right)/SOC\left(g\,C\,kg\,soil^{-1}\right) \times 100 \quad (5)$$

These conversions result in depth profiles of parameters presented in two ways: (i) depth profiles with soil layers defined by fixed soil masses regarding stocks, and (ii) depth profiles with soil layers defined by fixed soil depths regarding concentrations or proportions.

We used the nonparametric Kruskal Wallis test to look for statistical differences in parameters in individual soil layers between the organic and conventional cropping systems, as some of the data did not follow the normal distribution (*compare_means* function of the *ggpubr* package; Kassambara, 2023). Using the same test, we investigated differences between the two types of land use, cropland and meadow. For cropland the average of conventional and organic neighboring plots was calculated as the mean per layer. To look for significant differences in concentrations or proportions between soil layers regardless of the treatment we used the Kruskal Wallis test with Dunn's test for multiple comparisons and the Bonferroni p-value adjustment method (*dunnTest* function of the *FSA* R package; Ogle et al., 2023). Different letters were assigned to soil layers to express statistically significant differences using the *cldList* function of the *rcompanion* package (Mangiafico, 2024).

Relationships between soil properties and indicators of SOC stabilization along the soil profile and in individual soil layers were estimated using the Spearman rank correlation. A principal component analysis (PCA) was used to demonstrate relationships between SOC stabilization indicators with projection of soil properties on the circle of correlations. A scree plot and Kaiser's criterion were used to choose the number of principal components, and the data was centered and scaled before performing the analysis (*prcomp* function of the *stats* package; R Core Team, 2023).

Finally, we calculated a relative depth and a relative land-use effect on SOC and the studied SOC stabilization indicators expressed as proportions. The relative depth effect was calculated by comparing parameter values measured in the topsoil (0–30 cm) and subsoil (30–70 cm) and the land-use effect by comparing parameter values in meadow and in cropland in the topsoil (0–30 cm), as shown in Equation (6).

$$Relative\ Depth\ \boldsymbol{or\ Land - use\ effect} = (fX\ in\ subsoil\ \boldsymbol{or\ cropland} - fX\ in\ topsoil\ \boldsymbol{or\ meadow})/fX\ in\ topsoil\ \boldsymbol{or\ meadow} \quad (6)$$

Similarly to Henneron et al. (2022), for isotopic indicators we calculated absolute differences instead as these were considered more intuitive (e.g., absolute depth effect for $\delta^{13}C = \delta^{13}C_{SUBSOIL} - \delta^{13}C_{TOPSOIL}$; given in ‰, as the original measurements, instead of % change of permille concentration) and because the expected relative differences were orders of magnitudes apart from the rest of the parameters.

Data processing, statistical analysis and figure preparation were performed within the "R" programming environment (version 4.3.1; R Core Team, 2023). For plotting, packages *dplyr* (Wickham et al., 2023), *ggpmisc* (Aphalo, 2023), *reshape2* (Wickham, 2007) and *ggplot2* (Wickham, 2016) were used. For the preparation of Fig. 1 Microsoft PowerPoint (version 2408) was used.

3. Results

3.1. Bulk SOC and isotopic indicators of SOC stabilization

Conversion from SOC concentration (Fig. 2a) to SOC stock according to the ESM method revealed that SOC stock was statistically significantly higher in the meadow compared to the cropland in the two topmost layers (Fig. 3a). The p-value associated with these, and all the statistically significant detected differences presented below was p = 0.0495. The apparent lower values in the top layer, observed for SOC stock but also for all the SOC pools presented below (Fig. 3a–e), were due to the lower soil mass contained in this layer (717 t ha^{-1}) compared to the two layers that follow (1073–1450 t ha^{-1}). This highlights why ESM stock profiles are appropriate for comparing differences between treatments

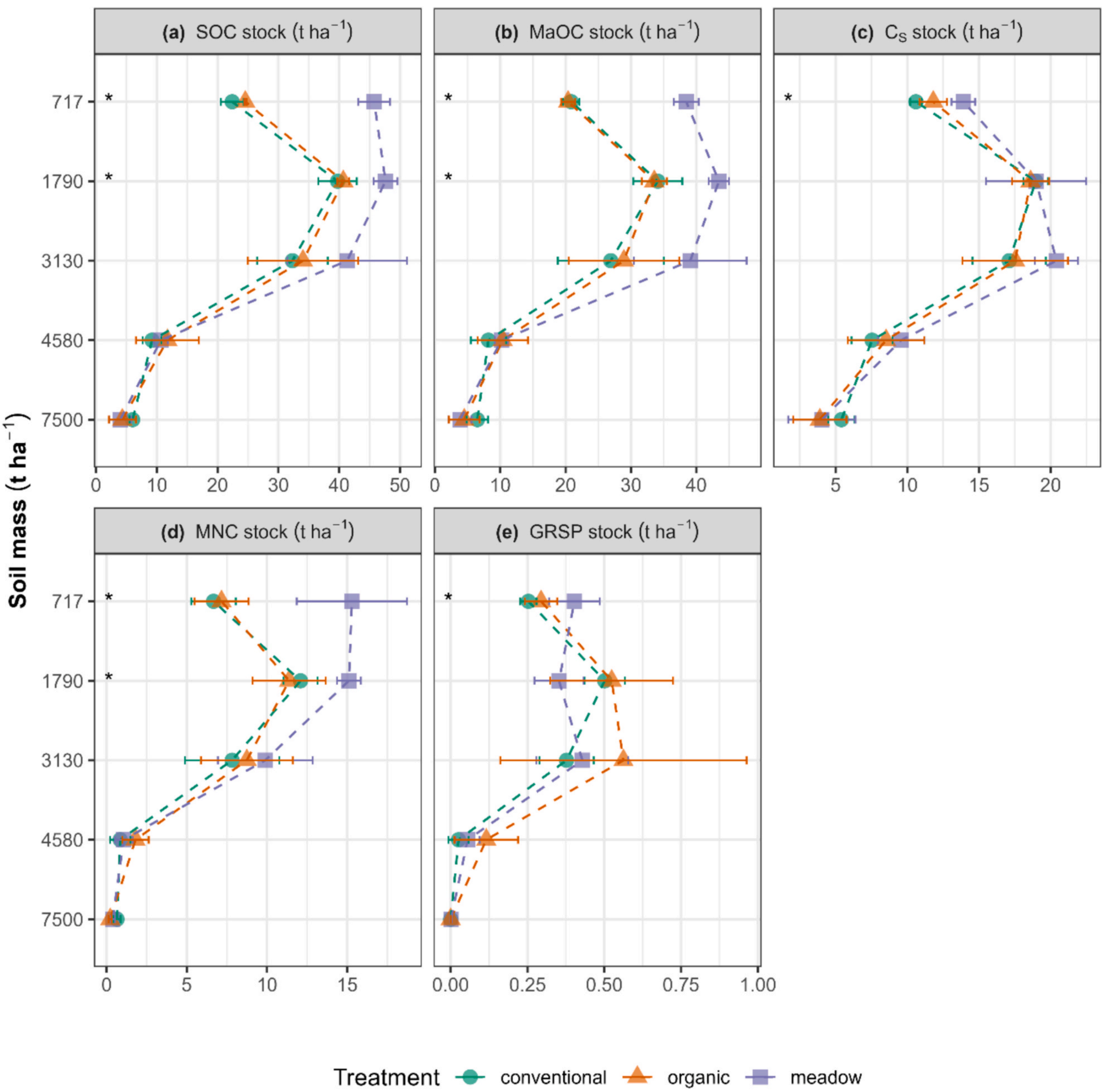

Fig. 3. a–e: Depth profiles of SOC, MaOC, C_S, MNC and GRSP as stocks according to the equivalent soil mass calculation method at the three treatments of the Yöni field experiment. Points represent mean values and error bars show the standard deviation (n = 3). Stars indicate statistically significant differences between the two land uses in each layer (p = 0.05).

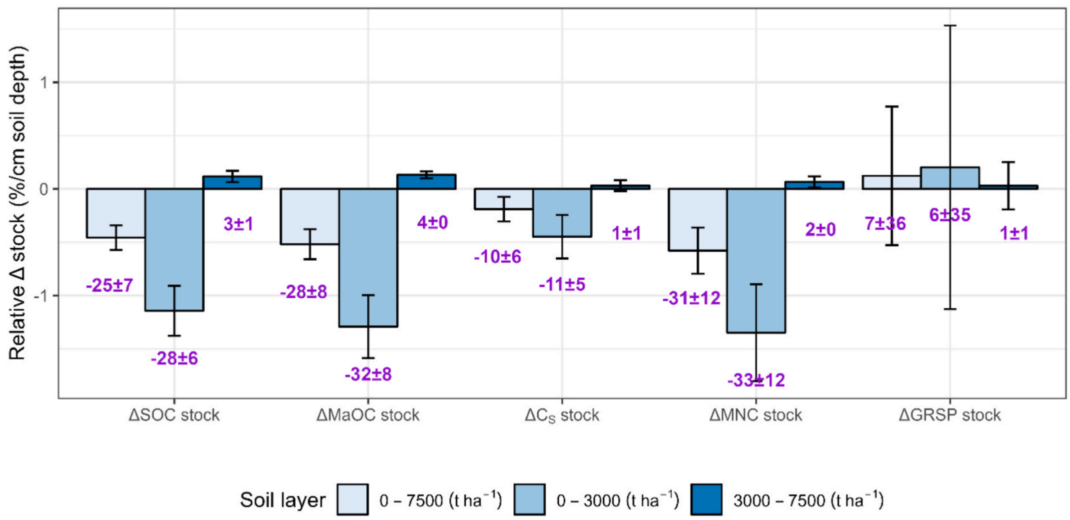

Fig. 4. Relative change in SOC, MaOC, C_S, MNC and GRSP stocks after conversion of grassland to cropland (using stocks of parameters measured in meadow as initial value). The three bars show the change in cumulative stocks, according to the equivalent soil mass calculation method, in the whole profile (light blue), topsoil (sky blue) and subsoil (dark blue). Numbers (in purple) indicate the mean change for each layer, while the bar heights, show the relative change per cm of soil depth, as indicated on the y-axis. Error bars show the standard deviation (n = 3). (For interpretation of the references to colour in this figure legend, the reader is referred to the web version of this article.)

but not suitable for studying changes in stocks with depth. Cumulatively, cropland had on average 25 ± 7 % lower SOC stock than the meadow considering the whole soil profile (Fig. 4). In the topsoil and subsoil (soil layers defined by soil mass 0–3000 t ha^{-1} and 3000–7500 t ha^{-1}, respectively), we observed a 28 ± 5 % decrease and a 3 ± 1 % increase, respectively, in the cropland compared to the meadow. Removing the effect of the different soil volumes by dividing the three soil layers by their height, showed that the relative difference between the two land uses was higher (~2.5 fold) in the topsoil compared to the whole soil profile.

SOC age defined by ^{14}C dating increased with depth in all three treatments (Fig. 2b). Depth profiles of mean SOC age were similar for the meadow and the organic cropping system, ranging from ~ 300 and ~ 600 years in the top (0–10 cm) layer to ~ 7,100 and ~ 7,800 years in the deepest (40–70 cm) layer for the two treatments, respectively. In the top layer in the conventional system, mean SOC age was similar to the organic system, with ~ 540 years but it reached ~ 9,500 years in the deepest layer, where the most pronounced and the only statistically significant difference was found between the two cropping systems. Differences in mean SOC age between the two land uses, cropland and meadow, were found to be statistically significant in the top and deepest layer.

The second isotopic indicator, $\delta^{13}C$ varied slightly along the soil profile (0.5 ‰) and showed similar trends in the conventional and organic system. However, values in two of the soil layers, the top (0–10 cm) and fourth (30–40 cm) layer, were statistically significantly less negative in the conventional cropping system (Fig. 2c). $\delta^{13}C$ values were more negative in the meadow in the surface layer reaching − 28.5 ‰, but they converged in all three treatments to − 27 ‰ in the deepest layer. Differences between cropland and meadow were found to be statistically significant in the four topmost soil layers (0–40 cm).

3.2. Physico-chemical indicators of SOC stabilization

Depth profiles of MaOC stock resembled the depth profiles of SOC stock (Figs. 3a and b) and were nearly identical between the two cropping systems, with no statistically significant differences in any of the studied soil layers. MaOC stock was highest in the second layer with 43 and 34 t ha^{-1} in the meadow and cropland, respectively, and decreased with depth reaching 4 and 5 t ha^{-1} in the deepest layer. In the meadow, MaOC stock was significantly higher than in the cropland in the two topmost layers. MaOC stock in cropland was on average 28 ± 8 % lower compared to the meadow considering the whole soil profile (Fig. 4). In the topsoil the difference was 32 ± 8 % and in the subsoil we observed a 4 % increase in the cropland. Removing the effect of the different soil volumes included in the three considered layers showed that the relative difference in MaOC between the two land uses was highest in the topsoil. The proportion of SOC present in the soil as MaOC was very high, with *f*MaOC values 91 % and 83 % in the top (0–10 cm) layer, in the conventional and organic cropping system, respectively. In the two cropland treatments *f*MaOC increased below 30 cm to 96 %. In the meadow, *f*MaOC increased from 84 % in the top layer, also to 96 % in the deepest (40–70 cm) layer. *f*MaOC in the meadow was significantly higher than in the cropland in the 10–20 and 20–30 cm layers but not in the 0–10 cm (Fig. 5a).

The C_S stock values were similar in the two cropping systems, with no statistically significant differences in any of the studied soil layers. In both cropland treatments, C_S stock was highest in the second layer with 19 t ha^{-1} and decreased with depth, reaching 5 t ha^{-1} in the deepest layer. In the meadow C_S stock reached its highest value in the third layer (20 t ha^{-1}) and was 4 t ha^{-1} in the deepest layer. C_S stock was significantly higher in the meadow compared to cropland only in the top layer (Fig. 3c). As a percentage difference, C_s stock was on average 10 ± 6 % lower in the cropland compared to the meadow, considering the whole soil profile (Fig. 4). This parameter also experienced the strongest change in the topsoil, with C_S stock 11 ± 5 % lower in the cropland compared to the meadow, while there was no change in the subsoil. Expressed as a proportion of SOC, fC_S strongly increased with depth in all treatments; from 47 % to 83 % in the cropland and from 30 % also to 83 % in the meadow (Fig. 5b). Significantly higher fC_S was found in the cropland compared to the meadow in the two topmost layers (0–10 and 10–20 cm).

3.3. Biochemical indicators of SOC stabilization

The MNC stock values showed no significant differences between the two cropping systems. In the cropland, the MNC stock was highest in the second layer (12 t ha^{-1}) and in the top layer in the meadow (15 t ha^{-1}). MNC stock decreased with depth in all treatments reaching 1 t ha^{-1} in the cropland and 0 t ha^{-1} in the meadow in the deepest layer (Fig. 3d).

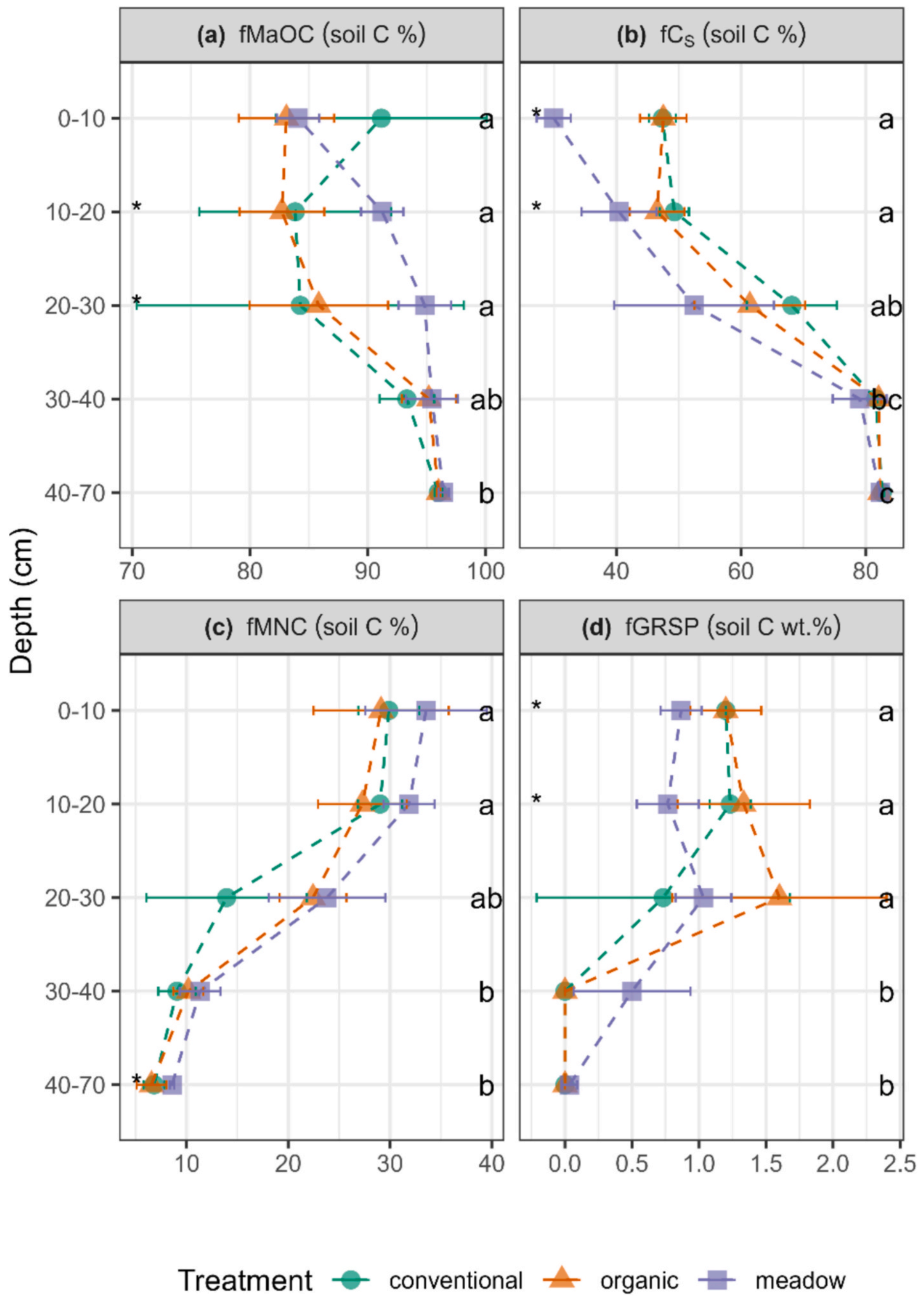

Fig. 5. a-d: Depth profiles of *f*MaOC, *f*C_S, *f*MNC (all given as SOC %) and *f*GRSP (wt. %) at the three treatments of the Yöni field experiment. Points represent mean values and error bars show the standard deviation (n = 3). Stars indicate statistically significant differences between the two land uses in each layer (Kruskal Wallis test; p = 0.05). Significant changes with depth regardless of the treatment are indicated by different letters (Kruskal Wallis and Dunn's test for multiple comparisons; p-values adjusted with the Bonferroni method).

Statistically significant MNC stock was found in the meadow compared to cropland in the two topmost layers. Amongst the studied parameters, MNC stock showed the highest relative difference between the two land uses, as it was on average 31 ± 12 % lower in the cropland compared to the meadow considering the whole soil profile, 33 ± 11 % lower in the topsoil and showed a slight increase of 2 ± 1 % the subsoil (Fig. 4). As a proportion of SOC, *f*MNC showed similar values and decreasing trend with depth in all treatments; from 30 % in the 0–10 cm layer to 7 % in the 40–70 cm layer in the two cropping systems and similarly from 34 % to 9 % in the meadow (Fig. 5c).

The stock of GRSP represented a much smaller amount in soil compared to the other fractions described above, reaching maximum values of 0.4 t ha^{-1} in the first and third layer in the meadow and 0.5 t ha^{-1} in the second layer in the cropland. GRSP stock decreased with depth to 0 t ha^{-1} in all treatments (Fig. 3e). There were no statistically significant differences between the two cropping systems while GRSP stock was statistically significantly higher in the meadow compared to the cropland in the top layer. The variability of the relative difference between the two land uses associated with GRSP stock was much larger than the observed means in all layers, with values of 7 ± 36 %, 6 ± 34 % 1 ± 2 % in the whole soil profile, topsoil and subsoil, respectively (Fig. 4). The calculated *f*GRSP was 1.2 wt% in the cropping systems and 0.9 wt% in the meadow 0–10 cm layer (Fig. 5d). *f*GRSP increased to 1.6 wt% in the organic system in the 20–30 cm layer and decreased to 0 in all treatments in the deepest layer. In the two topmost layers, 0–10 and 10–20 cm *f*GRSP was significantly higher in the cropland compared to the meadow.

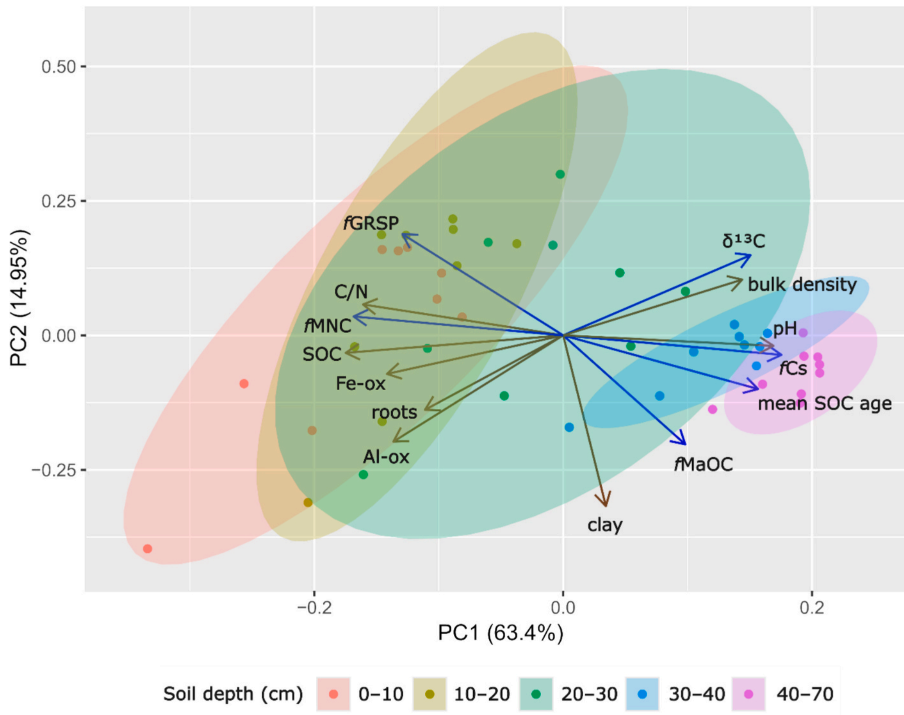

Fig. 6. Combination of loadings and biplots after a principal components analysis (PCA) including indicators of SOC stabilization (blue arrows) and soil properties (brown arrows). The ellipses were fitted to the PCA plane to include 95% of the points in each of the 5 sample depths. (For interpretation of the references to colour in this figure legend, the reader is referred to the web version of this article.)

3.4. Similarity amongst SOC stabilization indicators and relationship to soil properties

A principal component analysis (PCA), describing similarity amongst the various SOC stabilization indicators and their relationship to soil properties, showed that the first principal component (PC1) alone explained 64.4 % and together with the second (PC2) 80.5 % of the total variance (Fig. 6). PC1 separated soil samples mainly by soil depth and SOC content, as highlighted by the horizontal distribution of the ellipses and the strong association of SOC to negative values along PC1. Parameters increasing with depth had positive loadings along PC1 and those decreasing with depth showed negative loadings along the same component. Overlap of the ellipses representing the two topmost layers and the ellipses representing the two deepmost layers was indicative of similarity inside these two groupings. As they all increased with depth, mean SOC age and δ^{13}C were strongly and positively correlated to fC_s, while mean SOC age and fC_S were negatively correlated to the two biochemical indicators, *f*MNC and *f*GRSP. There was a strong positive correlation between the two biochemical indicators and strong negative correlations between δ^{13}C and *f*MNC and between *f*MaOC and *f*GRSP. Regarding soil properties, the two isotopic indicators and fC_S were negatively correlated to SOC content, C/N ratio and Fe-oxide concentration (all decreasing with depth; Table S1), while the two biochemical indicators showed positive correlations to the same properties, in addition to the Al-oxide concentration (also decreased in the deepest layer; Table S1). In contrast, δ^{13}C and fC_s were strongly negatively correlated to the concentration of Al-oxides, and *f*GRSP correlated strongly and positively to the C/N ratio. Mean SOC age, δ^{13}C and fC_s were positively correlated to pH (slight increase with depth, from 6 to 7.2; Table S1). In contrast, *f*MNC and *f*GRSP were strongly negatively correlated to pH. No significant strong correlation was observed between soil characteristics and *f*MaOC, other than positive correlation to clay content.

Because of the strong influence of depth on the SOC stabilization indicators, we investigated their similarity and their correlations to soil properties within each soil layer (Table 1).

We found a strong negative correlation between mean SOC age and *f*MNC in the 20–30 and 30–40 cm layer. There was a positive correlation between δ^{13}C and fC_s in the 0–10, 20–30 and 30–40 cm layer. δ^{13}C was negatively correlated to *f*MNC in the 10–20 cm layer and to *f*GRSP in the 30–40 cm layer. *f*GRSP was positively correlated to δ^{13}C in the 0–10 cm layer.

A few correlations between indicators of SOC stabilization and soil properties were repeatedly observed in all layers, such as the strong negative correlation of δ^{13}C and fC_s to SOC content and the strong negative correlation between δ^{13}C and Al-oxide concentration. In all layers except the 30–40, δ^{13}C was strongly negatively correlated to clay content and to the concentration of Fe-oxides. In all layers except the 0–10, δ^{13}C was strongly negatively correlated to C/N ratio and fC_S was strongly positively correlated to pH. A strong negative correlation of fC_S to the C/N ratio and to the Al-oxide concentration was found in the 20–30 and 30–40 cm layers, and fC_S was strongly negatively correlated to clay content in the 0–10 and 30–40 cm layers. Some correlations were occurring only in single layers, namely a strong positive correlation of δ^{13}C to pH in the 20–30 cm layer, and a strong positive correlation of *f*MNC to the C/N ratio and to SOC content in the 10–20 and 20–30 cm layer, respectively. The correlation of *f*GRSP to SOC, Al-oxide concentration and clay content, changed from strong positive in the 0–10 layer to strong negative in the 30–40 cm layer. Additionally, in the 30–40 cm layer there was the only occurrence of a strong positive correlation of *f*GRSP to C/N ratio and Fe-oxide concentration and a strong negative correlation to pH.

4. Discussion

Biogeochemical stability of SOC has been shown to increase as SOC content decreases following the conversion of grassland to cropland. Furthermore, turnover and decomposition of SOC have been shown to slow down with increasing depth (Hobley et al., 2017; Poeplau and Don, 2013). Indicators used to describe pools of SOC with higher potential for

Table 1
Correlations between soil properties and (amongst) stable SOC indicators in separate soil layers including all treatments. High (ρ > 0.6) and significant ($p < 0.05$) correlations are marked in bold. The significance levels are indicated as: *** for $p < 0.001$, ** for $p < 0.01$ and * for $p < 0.05$.

Layer 0–10 cm

	mean SOC age (years BP)	**$\delta^{13}C$ (‰)**	***f*C$_S$ (soil C %)**	***f*MaOC (soil C %)**	***f*GRSP (wt. %)**	***f*MNC (soil C %)**
SOC (%)	−0.544	**−0.914** ***	**−0.967** ***	−0.33	**−0.756** *	0.504
C/N	0.206	−0.647	−0.516	−0.277	−0.171	0.491
pH	0.261	0.193	0.547	0.014	0.146	−0.642
Clay (%)	−0.473	**−0.956** ***	**−0.810** **	−0.078	**−0.853** **	0.422
Al-ox (mg kg soil^{-1})	−0.098	**−0.798** **	−0.556	−0.28	**−0.939** ***	0.326
Fe-ox (mg kg soil^{-1})	−0.054	**−0.867** **	−0.625	−0.245	−0.657	0.384
mean SOC age (years BP)		0.344	0.609	−0.242	0.35	−0.37
$\delta^{13}C$ (‰)			**0.851** **	0.276	**0.770** *	−0.417
*f*C$_S$ (soil C %)				0.267	0.604	−0.593
*f*MaOC (soil C %)					0.224	0.033
GRSP:SOC (mg / mg C)						−0.217

Layer 10–20 cm

	mean SOC age (years BP)	**$\delta^{13}C$ (‰)**	***f*C$_S$ (soil C %)**	***f*MaOC (soil C %)**	***f*GRSP (wt. %)**	***f*MNC (soil C %)**
SOC (%)	−0.142	**−0.786** *	**−0.699** *	0.522	−0.502	0.427
C/N	−0.558	**−0.715** *	−0.578	0.661	−0.321	**0.827** **
pH	0.537	0.096	**0.739** *	−0.28	0.041	−0.22
Clay (%)	0.016	**−0.954** ***	−0.352	0.64	**−0.724** *	0.651
Al-ox (mg kg soil^{-1})	−0.303	**−0.786** *	−0.421	0.476	−0.665	0.574
Fe-ox (mg kg soil^{-1})	−0.033	**−0.832** **	−0.525	0.644	−0.611	0.481
mean SOC age (years BP)		0.059	0.351	−0.139	−0.313	−0.471
$\delta^{13}C$ (‰)			0.345	−0.648	0.545	**−0.715** *
*f*C$_S$ (soil C %)				−0.529	0.087	−0.29
*f*MaOC (soil C %)					−0.231	0.52
GRSP:SOC (mg / mg C)						−0.058

Layer 20–30 cm

	mean SOC age (years BP)	**$\delta^{13}C$ (‰)**	***f*C$_S$ (soil C %)**	***f*MaOC (soil C %)**	***f*GRSP (wt. %)**	***f*MNC (soil C %)**
SOC (%)	−0.463	**−0.902** ***	**−0.923** ***	0.378	0.206	**0.667** *
C/N	0.002	**−0.684** *	**−0.725** *	−0.046	0.294	0.196
pH	0.199	**0.877** **	**0.789** *	−0.428	−0.036	−0.487
Clay (%)	−0.245	**−0.792** *	−0.339	0.536	−0.284	0.5
Al-ox (mg kg soil^{-1})	−0.358	**−0.930** ***	**−0.670** *	0.466	−0.133	0.647
Fe-ox (mg kg soil^{-1})	−0.07	**−0.825** **	−0.469	0.413	0.132	0.264
mean SOC age (years BP)		0.374	0.458	−0.315	−0.383	**−0.796** *
$\delta^{13}C$ (‰)			**0.756** *	−0.438	−0.147	−0.652
*f*C$_S$ (soil C %)				−0.044	−0.483	−0.608
*f*MaOC (soil C %)					−0.451	0.472
GRSP:SOC (mg / mg C)						0.199

Layer 30–40 cm

	mean SOC age (years BP)	**$\delta^{13}C$ (‰)**	***f*C$_S$ (soil C %)**	***f*MaOC (soil C %)**	***f*GRSP (wt. %)**	***f*MNC (soil C %)**
SOC (%)	−0.126	**−0.922** ***	**−0.974** ***	0.016	**0.746** *	−0.028
C/N	−0.188	**−0.866** **	**−0.937** ***	−0.059	**0.713** *	0.015
pH	0.077	0.621	**0.790** *	−0.055	**−0.844** **	−0.088
Clay (%)	−0.068	−0.586	−0.713*	0.284	**0.841** **	0.256
Al-ox (mg kg soil^{-1})	−0.063	**−0.757** *	**−0.817** **	0.129	**0.901** ***	0.021
Fe-ox (mg kg soil^{-1})	0.076	−0.397	−0.346	0.486	**0.921** ***	0.237
mean SOC age (years BP)		0.031	0.116	0.111	0.118	**−0.797** *
$\delta^{13}C$ (‰)			**0.887** **	−0.076	**−0.668** *	0.18
*f*C$_S$ (soil C %)				0.097	−0.642	0.134
*f*MaOC (soil C %)					0.405	0.169
GRSP (mg / mg C)						0.047

stabilization are based on different conceptual mechanisms (Lehmann and Kleber, 2015; Schmidt et al., 2011; von Lützow et al., 2006) and information on their intercomparison is lacking. Here, we studied the relationships between some of these indicators and their evolution after disturbance at the multi-decadal scale. Our initial hypotheses were partly confirmed, as (H1) the most influential factor controlling SOC stabilization indicators was soil depth, and the expected increase in SOC stabilization with depth was indeed reflected by the two isotopic indicators and *f*C$_S$ and also slightly by *f*MaOC. However, this was not the case for the amino sugar derived *f*MNC nor for *f*GRSP, whose contribution to total OC decreased with depth instead (Fig. 7). As expected, (H2) isotopic indicators and *f*C$_S$ indicated an increasing contribution of old/stabilized C to total SOC in the cropland compared to the meadow, associated with a decrease in fresh C inputs (Fig. 7). This was not the case for *f*MaOC, which changed in the opposite direction (Fig. 5a). Concerning the difference in biochemical indicators between the two land uses, we did not observe the expected (H3) decrease in the relative contribution of *f*MNC and *f*GRSP, comparing meadow to cropland. Instead, *f*MNC was similar amongst the two land uses and *f*GRSP changed in the opposite direction but with high uncertainties (Figs. 5c and d). The expected (H4) correlations of SOC stabilization indicators to clay content and metal oxides were observed but were mainly depth driven (Fig. 6). In individual layers, mainly the concentration of aluminum and iron oxides were consistently and strongly correlated to

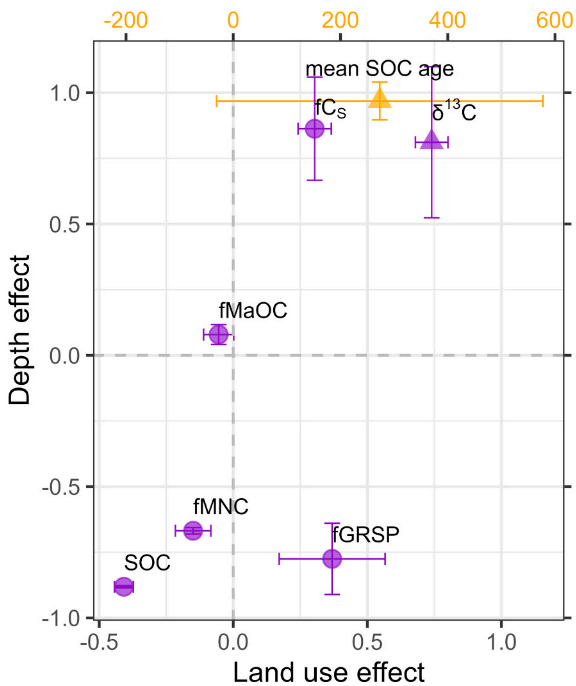

Fig. 7. Depth and land use effect on the different parameters. The depth effect was calculated by comparing parameter values measured in the topsoil (0–30 cm) and subsoil (30–70 cm) and using topsoil as a reference value, and the land-use effect by comparing parameter values in meadow and in cropland (average for conventional and organic treatment) in the topsoil (0–30 cm) and using meadow as a reference value. Circles indicate mean values of relative change (given in % for SOC, *f*MaOC, *f*C$_s$, and *f*MNC, and *f*GRSP) and triangles indicate mean values of absolute change (given in years for the mean SOC age and in ‰ points for δ^{13}C). Error bars show the standard deviation (n = 3). Notice the secondary x- and y- axes used for mean SOC age.

SOC stabilization assessed by δ^{13}C and *f*C$_S$.

4.1. Response of mean SOC age to changing land use and soil depth

Along the soil profile, SOC age increased by ~ 5,000 years on average for all treatments (Fig. 7) as expected, showing the increasing contribution of an older, more stable, soil organic matter fraction in deeper layers (Trumbore, 1997). The increase in SOC age in the cropland compared to the meadow (~ 250 years on average; Fig. 7) agreed with previous studies (Guo and Gifford, 2002; Jenkinson et al., 2008; Mathieu et al., 2015). In the conventional treatment, the loss of SOC along the soil profile combined with the observed older mean SOC age, indicated mineralization of younger, rather than older C, a trend already shown in Hobley et al. (2017) comparing native vegetation to cropland sites. In the meadow and in the organic system, the exact processes forming the mean SOC age profiles are difficult to decipher definitively as SOC age is strongly influenced not only by SOC mineralization but also by fresh C inputs (Trumbore, 2009). As manure and fresh plant-derived C inputs primarily affect the top 40 cm of soil (Skadell et al., 2023), these additions likely led to reduced SOC age within this depth. Deeper in the soil, the younger SOC age observed in the meadow and organic systems may reflect bioturbation-driven translocation (e.g., by earthworms) and partial accumulation of fresh SOC (Lorenz and Lal, 2005). Additionally, fresh OM inputs may trigger a priming effect, leading to the loss of older C (Henneron et al., 2022; Shahzad et al., 2018). Moreover, the detected difference in SOC age in the deepest layer between conventional cropping system and meadow (~ 2,400 years; Fig. 2), despite the uniform SOC concentration amongst treatments, supports the idea that the drivers of bulk SOC and SOC age may differ (Hobley et al., 2017). E.g., Mathieu et al. (2015) suggested that along the depth profile, drivers of SOC age are changing from climate and land use in the topsoil to soil texture and mineralogy in the subsoil. In our study, along the soil profile mean SOC age increased with decreasing SOC content, C/N ratio, and Fe-oxide concentration, and with increasing pH, but we did not find any significant correlations to any of the tested soil properties in the per-layer analysis. The steep increase in SOC age in the 40–70 cm layer across all treatments aligns with findings from Ultuna (SE) by (Menichetti et al., 2015), who reported a rise from ~ 1,800 ± 300 years (40–60 cm) to ~ 7,800 ± 100 years below 60 cm, likely due to the pre-terrestrial origin of SOC in the deepest layer. This would be a sound assumption for our study site, since the age of this clay soil (deposited in deep water) aligns well with deglaciation and sedimentation in this area estimated between ~ 9,800 and ~ 8,300 years ago (Sauramo, 1923 and Kankainen, 1993 cited in Salminen et al., 1997).

4.2. Response of δ^{13}C signature to changing land use and soil depth

The measured δ^{13}C values were in the expected range for a pure C3 vegetation site. The shift caused in the δ^{13}C signature by land use was on average 0.75 ‰ in the topsoil and the increase with depth on average for all treatments was 0.7 ‰ (Fig. 7). For reference, average values recorded in German topsoils were −28.2 ‰ and −26.8 ‰ under grassland and cropland, respectively (Schneider et al., 2021), and a similar increase, in the order of 1.5–2.0 ‰ was observed by Hobley et al. (2017) in topsoil (10 cm) in cropland compared to grassland. The expected enrichment of ^{13}C with depth and thus increase in δ^{13}C signature was evident in all treatments but most pronounced in the meadow. This was also in agreement with previous studies, showing that the average increase to 80 cm depth was 1.5 ‰ in grassland and 0.7 ‰ in cropland (Krüger et al., 2024; Schneider et al., 2021). The steep δ^{13}C depth gradient observed in the meadow (untilled soil) and mostly evident in the first 30 cm, could be explained by the continuous fresh C inputs through the permanent vegetation cover (^{13}C-depleted relative to bulk SOC) and the Suess effect, the depletion of modern atmospheric CO_2 in ^{13}C that can be in the order of 2 ‰ (Krüger et al., 2024). The minimal gradient of δ^{13}C change with depth in the cropping systems could be caused by the removal of biomass through harvest (Smith et al., 2007). In all cases, enrichment of the heavier ^{13}C isotope, discriminated against during microbial processing, could also be acting in parallel, increasing δ^{13}C signature with depth in all treatments (Henneron et al., 2022; Hou et al., 2019; Krüger et al., 2024). The distribution of microbial necromass in the soil column has also been proposed as a main driver of the δ^{13}C profile, due to its higher ^{13}C concentration compared to the plant biomass (Ehleringer et al., 2000; Ni et al., 2020). In our site, this could be a relevant driver, in line with the observed δ^{13}C enrichment with depth. Nonetheless, this was not reflected by the relative contribution of *f*MNC to SOC, which decreased with depth. Finally, Kohl et al. (2015) suggested that an increase in bacterial relative to fungal biomass with depth is an important driver of the vertical δ^{13}C gradient. However, in our study we found a decrease in the ratio of bacterial to fungal necromass with depth (Fig. S2) and an opposite (negative) correlation between the two indicators, possibly due to the drastically different methods used to quantify bacterial and fungal derived SOC (individual phospholipid fatty acids in Kohl et al. (2015) vs. amino sugars in our study). In our study, δ^{13}C was the indicator with the most correlations to soil properties in individual soil layers. In multiple soil layers, δ^{13}C was strongly and negatively correlated to SOC, C/N ratio, clay content and Al- and Fe-oxide content. These correlations can be explained by the strong land use effect on this parameter and the somewhat different soil properties of the meadow soil profile compared to the cropland (Table S1). The significantly higher fresh C inputs observed in meadow compared to the cropland were responsible for decreasing its δ^{13}C signature, while the land use change (compaction) resulted in topsoil layers with e.g., a higher clay and Al-oxide content in the meadow compared to the cropland, explaining the strong negative correlations between δ^{13}C and these soil properties.

4.3. Response of centennially persistent carbon to changing land use and soil depth

Along the soil profile, the proportion of centennially stable SOC derived by thermal analysis and the $PARTY_{SOC}$ model, fC_S, increased with depth as expected (by ∼ 75 % on average independently of treatment; Fig. 7) and as shown before (Kanari et al., 2021; Soucémarianadin et al., 2018). More than just a reduced influence of fresh C inputs with depth, processes linked to the increase in thermal stability with depth reported in literature include slower respiration (Soucémarianadin et al., 2018) and poor 'return-on-energy-investment' for decomposers (defined as the difference between the activation energy of decomposition and the energy density of a compound) in deeper soil layers (Henneron et al., 2022). fC_S measured under the two land uses followed the expected trend as well (increase in cropland topsoil by ∼ 27 % compared to meadow; Fig. 7). This was also observed by Delahaie et al. (2024) at the scale of France, with 38 % in grassland and 52 % fC_S in cropland topsoils. In our study, in the topsoil, the stock of C_S was 10 % lower in cropland compared to the meadow (Fig. 4), although in theory this content is expected to be an ecosystem property, affected more strongly by pedoclimatic parameters and historical land use than current land management (Barré et al., 2010; Cécillon et al., 2021). A similar trend was observed by Schiedung et al. (2025) and Delahaie et al. (2024) who reported lower C_S concentrations in cropland compared to grassland (accounting for approx. 15 and 25 g C kg soil^{-1} in German cropland and grassland, respectively and 8.4 and 11.5 g C kg soil^{-1} in French cropland and grassland). However, in both of those studies, the C_S concentrations were not corrected to ESM stocks, which could explain at least part of the difference. In addition, changes observed for the C_S concentration after land use change from grassland to cropland were shown to be indeed less important than for bulk SOC in the study by Schiedung et al. (2025). Two possible explanations for the lower C_S stocks in cropland in our study include: (i) the important uncertainty (6 %; in the same order of magnitude as the observed mean; Fig. 4) associated with this difference and (ii) some possible uncertainty associated with the predicted C_S concentrations due to the fact that our dataset crosses the limits of the calibration set of the model used to predict the size of this pool with respect to some soil characteristics (i.e., soil depth, SOC range, clay content range, and predicted C_S content range; Cécillon et al., 2021). Importantly, changes recorded along the soil profile for the content of the centennially active SOC pool (C_A) quantified by the same method (defined as C_A (g C kg soil^{-1}) = SOC − C_S; Fig. S3) were indeed of a much higher amplitude than for C_S, confirming the more stable nature of this pool compared to bulk SOC.

The predicted values for the concentration of C_S were higher in our study site than in French cropland and grassland. The higher overall values could indicate a higher amount of stabilized SOC in the Nordic pedoclimate but should be interpreted with caution for the reasons stated above. Theoretically, the lower temperatures, very high clay content and concentration of Al- and Fe-oxides could support the formation of a larger pool of stabilized SOC. Here, correlations between fC_S and soil properties observed in individual soil layers showed that the contribution of fC_S indeed increased as $\delta^{13}C$ indicated fewer fresh inputs, with increasing pH and counter-intuitively, with decreasing clay content. The negative correlation between the size of the clay fraction and fC_S is likely at least partly due to the lower clay content in the cropland soil, which also has lower SOC and is enriched in fC_S.

4.4. Response of mineral associated organic carbon to changing land use and soil depth

The slight increase in *f*MAOC with depth aligns with Georgiou et al. (2022) and Henneron et al. (2022), who predicted a similar vertical enrichment of about 6 %. However, the expected enrichment of *f*MaOC in the cropland compared to the meadow (Begill et al., 2023; Delahaie et al., 2024; Georgiou et al., 2022; Schiedung et al., 2025) was not observed in our study. Typically, grasslands accumulate up to twice more POC than croplands, due to higher amounts of plant litter entering the soil and the absence of tillage that can increase decomposition of soil organic matter (Grandy and Neff, 2008; Janzen et al., 2022; Sokol et al., 2022). In theory, conversion of grassland to cropland is associated to losses of labile carbon mainly through the POC pool, which leads to an enrichment in the contribution of *f*MaOC. Instead, in our study *f*MaOC was similar between the two land uses in the 0–10 cm layer (the only layer with a significantly higher POC in meadow than cropland; Fig. S3) and even decreased in the cropland compared to the meadow in the 10–30 cm soil layers. This decrease in *f*MaOC is explained by the similar POC concentration in these soil layers and by the very large fraction (up to 96 %) of SOC occurring as MaOC in this soil, meaning that SOC losses in cropland compared to meadow were associated to a strong decrease in the size of the MaOC pool. The strong sensitivity of a significant fraction (∼50 %) of MaOC to land use change is supported by recent studies (Anuo et al., 2024; Schiedung et al, 2025). The higher MaOC stock in the meadow could be expected and explained by the high C inputs in this system as reported above, leading to higher microbial activity and soil OM transformation and accumulation (Cotrufo et al., 2013; Liang et al., 2017; Sokol et al., 2022). Our results show that changes in MAOC in cropped systems closely mirrored changes in total SOC (Fig. 4), consistent with findings by Schiedung et al. (2025) in German grassland-to-cropland conversion sites. This supports the view that not all mineral association protects SOC from decay. Begill et al. (2023) describe MaOC accumulation in soil with a skyscraper or "piling up" analogy, supported by findings based on nano-scale imaging techniques (Schweizer, 2022; Vogel et al., 2014). Similarly, Kleber et al. (2007) stated that adsorbed organic molecules on mineral surfaces could be divided in different zones, resulting in various stabilization intensities. In our study, the strongest correlation found between *f*MaOC and soil properties was to clay content, but was depth driven. Otherwise, *f*MaOC was decoupled from any mineralogical or textural differences in individual layers.

4.5. Response of microbial necromass carbon to changing land use and soil depth

As a proportion of SOC, contrary to our initial hypothesis, *f*MNC was similar amongst the two land uses and accounted for 20–30 % of SOC in topsoils. This was also observed by Khan et al. (2016) reporting somewhat higher (50 % of SOC) but similar contribution of microbial necromass to SOC in cropland and grassland soils. Other studies found that *f*MNC was higher in grassland compared to cropland (Appuhn et al., 2006; Yang et al., 2022). This trend was indeed evident in our study regarding the concentration of MNC in topsoil, but not its relative proportion to SOC, suggesting that C inputs are the main driver for amino sugar production, while drivers of their stabilization may be more complex. Contrary to our initial hypothesis, we observed a decline in the relative proportion of *f*MNC with depth in all treatments (Fig. 7). We found conflicting evidence regarding the expected depth gradient of this fraction in previous studies. In an evaluation of global amino sugar distribution based on 131 soil profiles, Ni et al. (2020) observed a decline regarding amino sugar C concentration but an increase with depth when expressed as a proportion of SOC. Yet, this observation was made comparing the litter layer and the O-horizon to mineral soil (pooling forest, grassland and cropland soils). The same study presents unchanged *f*MNC with depth amongst the four layers representing the top 1 m of mineral soil. Also grouping together forest, grassland and cropland soils, Joergensen and Meyer (1990) mention a very slight but increasing trend in the proportion of amino sugar derived SOC with depth in the subsoil (18–46 cm). Results from Ding et al. (2019) suggest that depth (0–50 cm) has no influence on *f*MNC proportion, while Appuhn et al. (2006) reported a decrease in *f*MNC with depth and underlined that nevertheless the assessed mean residence time of SOC was following the opposite trend (increasing with depth). Struecker & Joergensen (2015), observing contrasting trends in the proportion of *f*MNC with depth in two arable sites with variable SOC content, have suggested that other factors may be forming the amino sugar distribution profile, such as nutrient limitation (C, N) rather than long-term preservation. Another possible reason hindering necromass accumulation in the studied soil could be its very high clay content. In the above-mentioned global analysis, Ni et al. (2020) observed that above the threshold value of 40 % clay, both the concentration and proportion of MNC were strongly reduced. They suggest that soils with finer texture could be creating an oxygen-limited environment hindering microbial anabolism and thus production and accumulation of microbial necromass. The only strong significant (positive) correlations of *f*MNC to soil properties observed in individual soil layers in our study were to SOC and C/N and limited to topsoil. Correlations with other indicators in the subsoil showed that SOC age increased with decreasing *f*MNC, and in the topsoil, *f*MNC increased with decreasing δ^{13}C (i.e., with increasing influence of fresh C inputs), all supporting that *f*MNC increased with additional inputs and not with SOC stabilization.

4.6. Response of glomalin-related soil proteins to changing land use and soil depth

As a mass proportion of SOC, contrary to our initial hypothesis, *f*GRSP was lower in the meadow than the cropland (Fig. 7) and accounted for 0.7–1.5 wt% of SOC in the top 30 cm. We found contrasting evidence in literature regarding the influence of land use on *f*GRSP, with studies reporting higher *f*GRSP under grassland compared to cropland (Zhao et al., 2025), the opposite trend (Huang et al., 2021; Staunton et al., 2020), or even similar contributions of *f*GRSP in the two land uses (Nautiyal et al., 2019). Although the evidence is not conclusive regarding the proportion of *f*GRSP, in theory, GRSP concentration in native ecosystems is expected to be higher. This hypothesis assumes that GRSP is mainly a product of arbuscular mycorrhizal fungi (AMF), which should thrive in undisturbed environments, and are sensitive to agronomical practices such as tillage and the use of fertilizers, herbicides and pesticides (Oehl et al., 2003; Staunton et al., 2020). Staunton et al. (2020) interpret the lack of sensitivity of GRSP content to land use as a decoupling between this concentration and AMF activity, suggesting there may be other sources for its origin. Similarly, Cissé et al. (2021) argue that GRSP may be introduced in the soil from different sources of organic matter, including manure, root exudates, or crop residues. Considering the large uncertainty associated with the relative change observed in this parameter between the two land uses (Fig. 4) and its multiple drivers described above, the slight differences we observed here are difficult to interpret. Regarding the evolution of *f*GRSP with depth, in our study we observed a decline in all treatments (Fig. 7). We found contrasting evidence in literature regarding the evolution of *f*GRSP in deeper soils. Numerous studies showed either an increase in *f*GRSP with depth (Cissé et al., 2023; Rillig et al., 2001; Wang et al., 2017), or indicated the opposite trend (Rillig et al., 2003; Woignier et al., 2014), while others even found an unchanged *f*GRSP with soil depth (Nautiyal et al., 2019). One possible explanation could be the large variation associated with this parameter (2–3 times the observed mean) presented in Wang et al. (2017) for 72 cropland soils as well as in our study. Alternatively, following the argument presented by Cissé et al. (2021) lack of accumulation of GRSP could be caused, as discussed above for MNC, by nutrient availability.

4.7. On the variety of SOC stabilization indicators, their limitations and potential

As, due to the complexity of the system and the interaction of multiple biotic and abiotic factors forming SOC stabilization, it is impossible to directly measure this attribute (Lehmann et al., 2020; Schmidt et al., 2011), research relies on developed proxies. Even though cycling of SOC is occurring on a wide spectrum of timescales, for the purpose of this discussion we use the simplified view that defines SOC as belonging either to an "active" or a "stable" pool, with mean residence times shorter or longer than 30 years, respectively. We consider this an appropriate division as it reflects observations from long-term field experiments (excluding the small and very fast cycling C pool with turnover time less than a year; Balesdent et al., 1987; Lavallee et al., 2020) and is a relevant time scale for studying the impact of disturbance (Poeplau and Don, 2013).

Radiocarbon dating is a powerful tool for assessing the age of SOC, not equal but closely related to its stabilization (Six and Jastrow, 2002), capturing changes occurring at time scales from decades to thousands of years. Mean SOC age is the average of very young and very old SOC present in the soil (Torn et al., 2009), while predicting changes in SOC requires a separation into pools with different kinetics (Trumbore, 2000) that is subject to equifinality if both the sizes of the pools and their turnover times are unknown. Similarly, δ^{13}C has great potential to infer SOC dynamics when used as a tracer in laboratory or field labelling experiments (Mary et al., 2020; Rasse et al., 2006), but without manipulation (labelling or vegetation change chrono sequence) and without consideration of kinetic pools, changes in this indicator are the result of multiple fluxes (Krüger et al., 2024). This was also the case in our study, meaning that in this setup both isotopic indicators can describe the relative composition of SOC (i.e., containing more, or less fresh, or young SOC as opposed to older SOC) and are useful for comparing land uses and depths layers, but they do not provide information on absolute SOC kinetics.

Physico-chemical indicators are on the rise as cheap, high throughput methods, important for modelling studies-since they are used to separate SOC in kinetic pools. Thermal stability is a powerful proxy of biogeochemical stability of SOC, and combined with the PARTY$_{SOC}$ model, it has the advantage of estimating the size of the centennially stable SOC pool (Cécillon et al., 2018, 2021). As this method was calibrated on sites where the size of this pool could be estimated (long term bare fallows; Barré et al., 2010), the quantified pool is less susceptible to changes at the relevant time scale (confirmed also in agronomic experiments including plants; Kanari et al., 2022). This approach combined with operational SOC models is valuable for predicting SOC changes at the scale of multiple decades and informing policy makers (Kanari et al., 2022). This method has been criticized for the lack of mechanistic understanding it provides, although recently progress has been made in this respect (Henneron et al., 2022). The validity of this approach is supported also by strong observed links to other methods including ^{14}C, differential scanning calorimetry and infrared spectroscopy (Barré et al., 2016; Plante et al., 2013; Sanderman and Grandy, 2020; Schiedung et al., 2025). A current limitation of this method before it can be more extensively used, is that the PARTY$_{SOC}$ model requires further calibration in other pedoclimates, land uses (forest soils) and depths. In contrast, mineral-associated OC is probably the most widely adopted indicator of SOC stabilization, with data available from various environments, soil types and land uses, since it has the important advantage of requiring little expertise or equipment to obtain. Support for the validity of this method comes from the concept of stabilization of organic matter through interaction with the mineral matrix (von Lützow et al., 2006), the observation that on a global scale MaOC has older mean ages than the coarser POC fraction (Cotrufo and Lavallee, 2022), a lower C/N ratio (Cotrufo et al., 2019) and a higher δ^{13}C signature (Poirier et al., 2005). Increasing evidence however shows that this separation is not sufficient to obtain a homogeneous pool regarding SOC mean residence time and that part of MaOC is actively cycling at the decadal scale (Balesdent, 1996; Balesdent et al., 1987; Jilling et al., 2025; Poeplau et al., 2023; Schiedung et al., 2025; Stoner et al., 2023; von Lützow et al., 2007). One theory explaining the heterogeneity of this pool suggests that different formation pathways exist leading to MaOC fractions with different transformation pasts and different properties (Sokol et al., 2022), while even since the conceptualization of this fractionation method it has been underlined that this dualistic separation is not selective enough to separate uniform fractions in terms of chemistry and turnover rates (Lavallee et al., 2020).

Certainly, biochemical indicators can help fill the knowledge gap regarding the processes behind SOC formation and stabilization. Amino sugars are suitable biomarkers for assessing the origin of soil organic matter, and empirical observations showing that older SOC has undergone microbial transformation (Derrien et al., 2023; Dynarski et al., 2020; Liang et al., 2019) are in support of the argument that these compounds can become stabilized in soil, e.g., through adsorption on mineral surfaces. To our knowledge, few studies have attempted to assess specifically the residence time of these compounds in soil, reporting variable estimations: from 4 years (Derrien and Amelung, 2011), to 6–90 years (Glaser et al., 2006), or 75–160 years (Liu et al., 2016). This is well in line with the idea that although it is not always the case, under specific conditions amino sugars can accumulate and persist. Similarly, originally, GRSP was not used as a proxy for SOC stabilization but as a potential tracer of AMF activity, that are considered important for soil aggregate formation (Agnihotri et al., 2021). Currently, the origin of this fraction is debated (Holátko et al., 2021; Staunton et al., 2020), while evidence of its longer mean residence time in soil is scarce. We found one study specifically assessing the residence time of this pool according to its ^{14}C content and a simple stock flow model, with estimations ranging from 6 to 42 years (Rillig et al., 2001). In addition, based on an incubation experiment, Rillig et al. (2003) support the idea that GRSP is only by 50 % in the active fraction because half of it was lost after 400 days. However, in the same experiment only 10 % of SOC was mineralized, meaning that as a proportion of OC, GRSP was reduced, i.e., it was lost faster than bulk OC. Moreover, the only study we could find investigating in-situ persistence of GRSP on the multidecadal scale concluded that there is no indication of preferential preservation of this fraction (Cissé et al., 2021).

5. Conclusions

Our study underlines that mean SOC age according to ^{14}C dating, $\delta^{13}C$ signature of bulk SOC and the proportion of centennially persistent OC derived from thermal analysis can capture changes in C inputs and intensity of disturbance between types of land use (cropland and meadow), as well as the expected depth effect on SOC stabilization in the top 40 cm of soil. On the contrary, in the studied system and time scale, the fraction of mineral-associated OC is as sensitive as bulk SOC to disturbance and is only slightly responsive to the depth effect. Regarding amino sugar derived microbial necromass C and glomalin-related soil proteins, we conclude that drivers of their production and stabilization are more complex than hypothesized, as they did not show any of the expected responses. Our study supports the use of isotopic and thermal indicators for the evaluation of SOC stabilization at the scale of multiple decades and we suggest that more research is needed to elucidate the interactions and processes defining the stabilization of the mineral associated OC and the studied biochemical compounds. To this end, carefully designed experiments combining multiple indicators hold great power.

CRediT authorship contribution statement

Eva Kanari: Writing – review & editing, Writing – original draft, Visualization, Investigation, Formal analysis, Conceptualization. **Kristiina Karhu:** Writing – review & editing, Investigation. **Anna-Reetta Salonen:** Writing – review & editing, Investigation. **Riitta Lemola:** Writing – review & editing, Investigation. **Helena Soinne:** Writing – review & editing, Investigation. **Pierre Barré:** Writing – review & editing, Investigation. **François Baudin:** Writing – review & editing, Investigation. **Kenichiro Mizohata:** Investigation. **Markku Oinonen:** Writing – review & editing, Investigation. **Jenie Gil:** Writing – review & editing, Investigation. **Lukas Kohl:** Writing – review & editing, Investigation. **Taina Pennanen:** Writing – review & editing, Investigation. **Chao Liang:** Writing – review & editing, Investigation. **Jussi Heinonsalo:** Writing – review & editing, Writing – original draft, Project administration, Funding acquisition, Conceptualization.

Declaration of competing interest

The authors declare that they have no known competing financial interests or personal relationships that could have appeared to influence the work reported in this paper.

Acknowledgements

The authors would like to thank Heli Antikainen, Kari Eskola, Anne-Maija Forss and Eero Tirkkonen for sample preparation for 14C-AMS analyses and Pietari Kienanen for the 14C-AMS analyses. We thank Aino Seppänen and Johanna Vielmaa for amino sugar analysis in the lab. The work of Pierre Barré and François Baudin as well as the amino sugar analyses were supported by the FREACS project funded by the external call of the EJP Soil (ANR-22-SOIL-0001). The work of Riitta Lemola, Taina Pennanen and Helena Soinne was funded by the Strategic Research Council (SRC) at the Research Council of Finland as part of the project ‘Multi-benefit solutions to climate-smart agriculture’ (MULTA, grant number 352435). This work was supported by the Strategic Research Council (grant no. 327342, 352431), Flagship funding (grant no. 337552) and research projects Deep-SOM (grant no. 340169) and Digi4CSA (grant no. 353073) all at the Research Council of Finland.

Appendix A. Supplementary data

Supplementary data to this article can be found online at https://doi.org/10.1016/j.geoderma.2025.117573.

Data availability

Data will be made available on request.

References

Agnihotri, R., Bharti, A., Ramesh, A., Prakash, A., Sharma, M.P., 2021. Glomalin related protein and C16:1ω5 PLFA associated with AM fungi as potential signatures for assessing the soil C sequestration under contrasting soil management practices. Eur. J. Soil Biol. 103. https://doi.org/10.1016/j.ejsobi.2021.103286.
Ahrens, B., Braakhekke, M.C., Guggenberger, G., Schrumpf, M., Reichstein, M., 2015. Contribution of sorption, DOC transport and microbial interactions to the 14C age of a soil organic carbon profile: Insights from a calibrated process model. Soil Biol. Biochem. 88, 390–402. https://doi.org/10.1016/J.SOILBIO.2015.06.008.
Angst, G., Mueller, K.E., Nierop, K.G.J., Simpson, M.J., 2021. Plant- or microbial-derived? A review on the molecular composition of stabilized soil organic matter. Soil Biol. Biochem. 156, 108189. https://doi.org/10.1016/J.SOILBIO.2021.108189.
Anuo, C.O., Sleem, M., Fossum, B., Li, L., Cooper, J.A., Malakar, A., Maharjan, B., Kaiser, M., 2024. Land use selectively impacts soil carbon storage in particulate, water-extractable, and mineral-associated forms across pedogenetic horizons. Geoderma 449, 116992. https://doi.org/10.1016/J.GEODERMA.2024.116992.
Aphalo, P.J., 2023. ggpmisc: Miscellaneous Extensions to ggplot2.
Appuhn, A., Joergensen, R.G., 2006. Microbial colonisation of roots as a function of plant species. Soil Biol. Biochem. 38, 1040–1051. https://doi.org/10.1016/j.soilbio.2005.09.002.
Appuhn, A., Scheller, E., Joergensen, R.G., 2006. Relationships between microbial indices in roots and silt loam soils forming a gradient in soil organic matter. Soil Biol. Biochem. 38, 2557–2564. https://doi.org/10.1016/j.soilbio.2006.03.011.
Balesdent, J., 1996. The significance of organic separates to carbon dynamics and its modelling in some cultivated soils. Eur. J. Soil Sci. 47, 485–493. https://doi.org/10.1111/j.1365-2389.1996.tb01848.x.
Balesdent, J., Basile-Doelsch, I., Chadoeuf, J., Cornu, S., Derrien, D., Fekiacova, Z., Hatté, C., 2018. Atmosphere–soil carbon transfer as a function of soil depth. Nature 559, 599–602. https://doi.org/10.1038/s41586-018-0328-3.
Balesdent, J., Mariotti, A., 1996. Measurement of soil organic matter turnover using 13C natural abundance. In: Boutton, T.W., Yamasaki, S.I. (Eds.), Mass Spectrometry of Soils. Marcel Dekker, New York, pp. 83–111.
Balesdent, J., Mariotti, A., Guillet, B., 1987. Natural 13C abundance as a tracer for studies of soil organic matter dynamics. Soil Biol. Biochem. 19, 25–30. https://doi.org/10.1016/0038-0717(87)90120-9.
Barré, P., Cécillon, L., Kanari, E., 2023. Characterization and evaluation of the stability of soil organic matter, in: Baudin, F. (Ed.), The Rock-Eval Method. pp. 181–207. https://doi.org/https://doi.org/10.1002/9781394256235.ch10.

Barré, P., Eglin, T., Christensen, B.T., Ciais, P., Houot, S., Kätterer, T., Van Oort, F., Peylin, P., Poulton, P.R., Romanenkov, V., Chenu, C., 2010. Quantifying and isolating stable soil organic carbon using long-term bare fallow experiments. Biogeosciences 7, 3839–3850. https://doi.org/10.5194/bg-7-3839-2010.

Barré, P., Plante, A.F., Cécillon, L., Lutfalla, S., Baudin, F., Bernard, S., Christensen, B.T., Eglin, T., Fernandez, J.M., Houot, S., Kätterer, T., Le Guillou, C., Macdonald, A., van Oort, F., Chenu, C., 2016. The energetic and chemical signatures of persistent soil organic matter. Biogeochemistry 130. https://doi.org/10.1007/s10533-016-0246-0.

Batjes, N.H., 1996. Total carbon and nitrogen in the soils of the world. Eur. J. Soil Sci. 65, 10–21. https://doi.org/10.1111/ejss.12114_2.

Begill, N., Don, A., Poeplau, C., 2023. No detectable upper limit of mineral-associated organic carbon in temperate agricultural soils. Glob. Chang. Biol. 29, 4662–4669. https://doi.org/10.1111/gcb.16804.

Bossio, D.A., Cook-Patton, S.C., Ellis, P.W., Fargione, J., Sanderman, J., Smith, P., Wood, S., Zomer, R.J., von Unger, M., Emmer, I.M., Griscom, B.W., 2020. The role of soil carbon in natural climate solutions. Nat Sustain 3, 391–398. https://doi.org/10.1038/s41893-020-0491-z.

Bronk Ramsey, C., 2009. Bayesian analysis of radiocarbon dates. Radiocarbon 51, 337–360. https://doi.org/DOI: 10.1017/S0033822200033865.

Cambardella, C.A., Elliott, E.T., 1992. Particulate soil organic-matter changes across a grassland cultivation sequence. Soil Sci. Soc. Am. J. 56, 777–783. https://doi.org/10.2136/sssaj1992.03615995005600030017x.

Carter, D.O., Yellowlees, D., Tibbett, M., 2007. Autoclaving kills soil microbes yet soil enzymes remain active. Pedobiologia (Jena) 51, 295–299. https://doi.org/10.1016/J.PEDOBI.2007.05.002.

Cécillon, L., 2021. lauric-cecillon/PARTYsoc: Second version of the PARTYsoc statistical model (Version v2.0). Zenodo.

Cécillon, L., Baudin, F., Chenu, C., Christensen, B.T., Franko, U., Houot, S., Kanari, E., Kätterer, T., Merbach, I., Van Oort, F., Poeplau, C., Quezada, J.C., Savignac, F., Soucémarianadin, L.N., Barré, P., 2021. Partitioning soil organic carbon into its centennially stable and active fractions with machine-learning models based on Rock-Eval® thermal analysis (PARTYSOCv2.0 and PARTYSOCv2.0EU). Geosci. Model Dev. 14, 3879–3898. https://doi.org/10.5194/gmd-14-3879-2021.

Cécillon, L., Baudin, F., Chenu, C., Houot, S., Jolivet, R., Kätterer, T., Lutfalla, S., Macdonald, A., Van Oort, F., Plante, A.F., Savignac, F., Soucémarianadin, L.N., Barré, P., 2018. A model based on Rock-Eval thermal analysis to quantify the size of the centennially persistent organic carbon pool in temperate soils. Biogeosciences 15, 2835–2849. https://doi.org/10.5194/bg-15-2835-2018.

Chen, Q., Shen, C., Sun, Y., Peng, S., Yi, W., Li, Z., Jiang, M., 2005. Spatial and temporal distribution of carbon isotopes in soil organic matter at the Dinghushan Biosphere Reserve, South China. Plant and Soil 273, 115–128. https://doi.org/10.1007/s11104-004-7245-y.

Chenu, C., Angers, D.A., Barré, P., Derrien, D., Arrouays, D., Balesdent, J., 2019. Increasing organic stocks in agricultural soils: Knowledge gaps and potential innovations. Soil Tillage Res. 188, 41–52. https://doi.org/10.1016/j.still.2018.04.011.

Chirol, C., Séré, G., Redon, P.-O., Chenu, C., Derrien, D., 2025. Depth dependence of soil organic carbon additional storage capacity in different soil types by the 2050 target for carbon neutrality. Soil 11, 149–174. https://doi.org/10.5194/soil-11-149-2025.

Cissé, G., Essi, M., Kedi, B., Nicolas, M., Staunton, S., 2023. Accumulation and vertical distribution of glomalin-related soil protein in French temperate forest soils as a function of tree type, climate and soil properties. Catena (Amst) 220. https://doi.org/10.1016/j.catena.2022.106635.

Cissé, G., van Oort, F., Chenu, C., Essi, M., Staunton, S., 2021. Is the operationally defined fraction of soil organic matter, "GRSP" (glomalin-related soil protein), stable in soils? Evidence from trends in long-term bare fallow soil. Eur. J. Soil Sci. 72, 1101–1112. https://doi.org/10.1111/ejss.12974.

Coplen, T.B., 2011. Guidelines and recommended terms for expression of stable-isotope-ratio and gas-ratio measurement results. Rapid Commun. Mass Spectrom. 25, 2538–2560. https://doi.org/10.1002/rcm.5129.

Cotrufo, M.F., Lavallee, J.M., 2022. Soil organic matter formation, persistence, and functioning: a synthesis of current understanding to inform its conservation and regeneration. In: Advances in Agronomy. Academic Press Inc., pp. 1–66. https://doi.org/10.1016/bs.agron.2021.11.002

Cotrufo, M.F., Ranalli, M.G., Haddix, M.L., Six, J., Lugato, E., 2019. Soil carbon storage informed by particulate and mineral-associated organic matter. Nat. Geosci. 12, 989–994. https://doi.org/10.1038/s41561-019-0484-6.

Cotrufo, M.F., Wallenstein, M.D., Boot, C.M., Denef, K., Paul, E., 2013. The Microbial Efficiency-Matrix Stabilization (MEMS) framework integrates plant litter decomposition with soil organic matter stabilization: do labile plant inputs form stable soil organic matter? Glob. Chang. Biol. 19, 988–995. https://doi.org/10.1111/gcb.12113.

Delahaie, A.A., Cécillon, L., Stojanova, M., Abiven, S., Arbelet, P., Arrouays, D., Baudin, F., Bispo, A., Boulonne, L., Chenu, C., Heinonsalo, J., Jolivet, C., Karhu, K., Martin, M., Pacini, L., Poeplau, C., Ratié, C., Roudier, P., Saby, N.P.A., Savignac, F., Barré, P., 2024. Investigating the complementarity of thermal and physical soil organic carbon fractions. Soil 10, 795–812. https://doi.org/10.5194/soil-10-795-2024.

Derrien, D., Amelung, W., 2011. Computing the mean residence time of soil carbon fractions using stable isotopes: Impacts of the model framework. Eur. J. Soil Sci. 62. https://doi.org/10.1111/j.1365-2389.2010.01333.x.

Derrien, D., Barré, P., Basile-Doelsch, I., Cécillon, L., Chabbi, A., Crème, A., Fontaine, S., Henneron, L., Janot, N., Lashermes, G., Quénéa, K., Rees, F., Dignac, M.F., 2023. Current controversies on mechanisms controlling soil carbon storage: implications for interactions with practitioners and policy-makers. A review. Agron Sustain Dev. https://doi.org/10.1007/s13593-023-00876-x.

Ding, X., Chen, S., Zhang, B., Liang, C., He, H., Horwath, W.R., 2019. Warming increases microbial residue contribution to soil organic carbon in an alpine meadow. Soil Biol. Biochem. 135, 13–19. https://doi.org/10.1016/j.soilbio.2019.04.004.

Ding, W., Sun, L., Fang, Y., Zvomuya, F., Liu, X., He, H., 2025. Depth-driven responses of soil organic carbon fractions to orchard cover crops across China: A meta-analysis. Soil Tillage Res 246, 106348. https://doi.org/10.1016/J.STILL.2024.106348.

Dynarski, K.A., Bossio, D.A., Scow, K.M., 2020. Dynamic stability of soil carbon: reassessing the "permanence" of soil carbon sequestration. Front. Environ. Sci. https://doi.org/10.3389/fenvs.2020.514701.

Ehleringer, J.R., Buchmann, N., Flanagan, L.B., 2000. Carbon isotope ratios in belowground carbon cycle processes. Ecol. Appl. https://doi.org/10.1890/1051-0761(2000)010[0412:CIRIBC]2.0.CO;2.

Ellert, B.H., Bettany, J.R., 1995. Calculation of organic matter and nutrients stored in soils under contrasting management regimes. Can. J. Soil Sci. 75, 529–538. https://doi.org/10.4141/cjss95-075.

Elzein, A., Balesdent, J., 1995. Mechanistic simulation of vertical distribution of carbon concentrations and residence times in Soils. Soil Sci. Soc. Am. J. 59, 1328–1335. https://doi.org/10.2136/sssaj1995.03615995005900050019x.

Emde, D., Poeplau, C., Don, A., Heilek, S., Schneider, F., 2024. The centennial legacy of land-use change on organic carbon stocks of German agricultural soils. Glob. Chang. Biol. 30, e17444. https://doi.org/10.1111/gcb.17444.

Engelking, B., Flessa, H., Joergensen, R.G., 2007. Shifts in amino sugar and ergosterol contents after addition of sucrose and cellulose to soil. Soil Biol. Biochem. 39, 2111–2118. https://doi.org/10.1016/j.soilbio.2007.03.020.

FAO, 2017. Soil Organic Carbon: the hidden potential., Food and Agriculture Organization of the United Nations. Rome, Italy. https://doi.org/10.1038/nrg2350.

FAO & ITPS, 2015. Intergovernmental Technical Panel on Soils. Status of the World's Soil Resources., Intergovernmental Technical Panel on Soils.

Faust, S., Heinze, S., Ngosong, C., Sradnick, A., Oltmanns, M., Raupp, J., Geisseler, D., Joergensen, R.G., 2017. Effect of biodynamic soil amendments on microbial communities in comparison with inorganic fertilization. Appl. Soil Ecol. 114, 82–89. https://doi.org/10.1016/J.APSOIL.2017.03.006.

Ferchaud, F., Chlebowski, F., Mary, B., 2023. SimpleESM : R script to calculate soil organic carbon and nitrogen stocks at Equivalent Soil Mass.

Friedlingstein, P., O'Sullivan, M., Jones, M.W., Andrew, R.M., Bakker, D.C.E., Hauck, J., Landschützer, P., Le Quéré, C., Luijkx, I.T., Peters, G.P., Peters, W., Pongratz, J., Schwingshackl, C., Sitch, S., Canadell, J.G., Ciais, P., Jackson, R.B., Alin, S.R., Anthoni, P., Barbero, L., Bates, N.R., Becker, M., Bellouin, N., Decharme, B., Bopp, L., Brasika, I.B.M., Cadule, P., Chamberlain, M.A., Chandra, N., Chau, T.T.T., Chevallier, F., Chini, L.P., Cronin, M., Dou, X., Enyo, K., Evans, W., Falk, S., Feely, R. A., Feng, L., Ford, D.J., Gasser, T., Ghattas, J., Gkritzalis, T., Grassi, G., Gregor, L., Gruber, N., Gürses, Ö., Harris, I., Hefner, M., Heinke, J., Houghton, R.A., Hurtt, G.C., Iida, Y., Ilyina, T., Jacobson, A.R., Jain, A., Jarníková, T., Jersild, A., Jiang, F., Jin, Z., Joos, F., Kato, E., Keeling, R.F., Kennedy, D., Goldewijk, K.K., Knauer, J., Korsbakken, J.I., Körtzinger, A., Lan, X., Lefèvre, N., Li, H., Liu, J., Liu, Z., Ma, L., Marland, G., Mayot, N., McGuire, P.C., McKinley, G.A., Meyer, G., Morgan, E.J., Munro, D.R., Nakaoka, S.I., Niwa, Y., O'Brien, K.M., Olsen, A., Omar, A.M., Ono, T., Paulsen, M., Pierrot, D., Pocock, K., Poulter, B., Powis, C.M., Rehder, G., Resplandy, L., Robertson, E., Rödenbeck, C., Rosan, T.M., Schwinger, J., Séférian, R., Smallman, T.L., Smith, S.M., Sospedra-Alfonso, R., Sun, Q., Sutton, A.J., Sweeney, C., Takao, S., Tans, P.P., Tian, H., Tilbrook, B., Tsujino, H., Tubiello, F., van der Werf, G. R., van Ooijen, E., Wanninkhof, R., Watanabe, M., Wimart-Rousseau, C., Yang, D., Yang, X., Yuan, W., Yue, X., Zaehle, S., Zeng, J., Zheng, B., 2023. Global carbon budget 2023. Earth Syst. Sci. Data 15. https://doi.org/10.5194/essd-15-5301-2023.

Georgiou, K., Jackson, R.B., Vindušková, O., Abramoff, R.Z., Ahlström, A., Feng, W., Harden, J.W., Pellegrini, A.F.A., Polley, H.W., Soong, J.L., Riley, W.J., Torn, M.S., 2022. Global stocks and capacity of mineral-associated soil organic carbon. Nat. Commun. 13, 3797. https://doi.org/10.1038/s41467-022-31540-9.

Glaser, B., Millar, N., Blum, H., 2006. Sequestration and turnover of bacterial- and fungal-derived carbon in a temperate grassland soil under long-term elevated atmospheric pCO2. Glob. Chang. Biol. 12. https://doi.org/10.1111/j.1365-2486.2006.01186.x.

Grandy, A.S., Neff, J.C., 2008. Molecular C dynamics downstream: the biochemical decomposition sequence and its impact on soil organic matter structure and function. Sci. Total Environ. 404, 297–307. https://doi.org/10.1016/J.SCITOTENV.2007.11.013.

Gregorich, E.G., Gillespie, A.W., Beare, M.H., Curtin, D., Sanei, H., Yanni, S.F., 2015. Evaluating biodegradability of soil organic matter by its thermal stability and chemical composition. Soil Biol. Biochem. 91, 182–191. https://doi.org/10.1016/j.soilbio.2015.08.032.

Gross, C.D., Harrison, R.B., 2019. The case for digging deeper: soil organic carbon storage, dynamics, and controls in our changing world. Soil Syst 3. https://doi.org/10.3390/soilsystems3020028.

Guan, X.-K., Turner, N.C., Song, L., Gu, Y.-J., Wang, T.-C., Li, F.-M., 2016. Soil carbon sequestration by three perennial legume pastures is greater in deeper soil layers than in the surface soil. Biogeosciences 13, 527–534. https://doi.org/10.5194/bg-13-527-2016.

Guo, L.B., Gifford, R.M., 2002. Soil carbon stocks and land use change a meta analysis - Guo - 2002 - Global Change Biology - Wiley Online Library. Glob. Chang. Biol. 8.

Gylden, C.W., 1850. Karta öfver Finland utvisande skogstillgångarna i landets särskilda delar år 1850 [WWW Document].

Heikkinen, J., Ketoja, E., Nuutinen, V., Regina, K., 2013. Declining trend of carbon in Finnish cropland soils in 1974-2009. Glob. Chang. Biol. 19, 1456–1469. https://doi.org/10.1111/gcb.12137.

Henneron, L., Balesdent, J., Alvarez, G., Barré, P., Baudin, F., Basile-Doelsch, I., Cécillon, L., Fernandez-Martinez, A., Hatté, C., Fontaine, S., 2022. Bioenergetic

control of soil carbon dynamics across depth. Nat. Commun. 13, 7676. https://doi.org/10.1038/s41467-022-34951-w.
Hicks Pries, C.E., Ryals, R., Zhu, B., Min, K., Cooper, A., Goldsmith, S., Pett-Ridge, J., Torn, M., Berhe, A.A., 2023. The Deep Soil Organic carbon response to global change. Annu. Rev. Ecol. Evol. Syst. https://doi.org/10.1146/annurev-ecolsys-102320-085332.
Hobley, E., Baldock, J., Hua, Q., Wilson, B., 2017. Land-use contrasts reveal instability of subsoil organic carbon. Glob. Chang. Biol. 23, 955–965. https://doi.org/10.1111/gcb.13379.
Holátko, J., Brtnický, M., Kučerík, J., Kotianová, M., Elbl, J., Kintl, A., Kynický, J., Benada, O., Datta, R., Jansa, J., 2021. Glomalin – Truths, myths, and the future of this elusive soil glycoprotein. Soil Biol. Biochem. https://doi.org/10.1016/j.soilbio.2020.108116.
Hou, Y., Chen, Y., Chen, X., He, K., Zhu, B., 2019. Changes in soil organic matter stability with depth in two alpine ecosystems on the Tibetan Plateau. Geoderma 351, 153–162. https://doi.org/10.1016/J.GEODERMA.2019.05.034.
Huang, J., Liu, W., Yang, S., Yang, L., Peng, Z., Deng, M., Xu, S., Zhang, B., Ahirwal, J., Liu, L., 2021. Plant carbon inputs through shoot, root, and mycorrhizal pathways affect soil organic carbon turnover differently. Soil Biol. Biochem. 160. https://doi.org/10.1016/j.soilbio.2021.108322.
Huang, X., Ibrahim, M.M., Luo, Y., Jiang, L., Chen, J., Hou, E., 2024. Land use change alters soil organic carbon: constrained global patterns and predictors. Earths. Future 12, e2023EF004254. https://doi.org/10.1029/2023EF004254.
IUSS Working Group WRB, 2015. World reference base for soil resources 2014, update 2015 International soil classification system for naming soils and creating legends for soil maps. World Soil Resources Reports No. 106. Rome.
Janzen, H.H., van Groenigen, K.J., Powlson, D.S., Schwinghamer, T., van Groenigen, J. W., 2022. Photosynthetic limits on carbon sequestration in croplands. Geoderma 416, 115810. https://doi.org/10.1016/J.GEODERMA.2022.115810.
Jenkinson, D.S., Coleman, K., 2008. The turnover of organic carbon in subsoils. Part 2. Modelling carbon turnover. Eur. J. Soil Sci. 59, 400–413. https://doi.org/10.1111/j.1365-2389.2008.01026.x.
Jenkinson, D.S., Poulton, P.R., Bryant, C., 2008. The turnover of organic carbon in subsoils. Part 1. Natural and bomb radiocarbon in soil profiles from the Rothamsted long-term field experiments. Eur. J. Soil Sci. 59, 391–399. https://doi.org/10.1111/j.1365-2389.2008.01025.x.
Jilling, A., Grandy, A.S., Daly, A.B., Hestrin, R., Possinger, A., Abramoff, R., Annis, M., Cates, A.M., Dynarski, K., Georgiou, K., Heckman, K., Keiluweit, M., Lang, A.K., Phillips, R.P., Rocci, K., Shabtai, I.A., Sokol, N.W., Whalen, E.D., 2025. Evidence for the existence and ecological relevance of fast-cycling mineral-associated organic matter. Commun. Earth Environ. 6, 690. https://doi.org/10.1038/s43247-025-02681-8.
Jobbagy, E.G., Jackson, R.B., 2000. The vertical distribution of soil organic carbon and its relation to climate and vegetation. Ecol. Appl. 10, 423–436.
Joergensen, R.G., Meyer, B., 1990. Chemical change in organic matter decomposing in and on a forest Rendzina under beech (Fagus sylvatica L.). J. Soil Sci. 41, 17–21. https://doi.org/10.1111/j.1365-2389.1990.tb00041.x.
Kanari, E., Barré, P., Baudin, F., Berthelot, A., Bouton, N., Gosselin, F., Soucémarianadin, L., Savignac, F., Cécillon, L., 2021. Predicting Rock-Eval® thermal analysis parameters of a soil layer based on samples from its sublayers; an experimental study on forest soils. Org Geochem. 160. https://doi.org/10.1016/j.orggeochem.2021.104289.
Kanari, E., Cécillon, L., Baudin, F., Clivot, H., Ferchaud, F., Houot, S., Levavasseur, F., Mary, B., Soucémarianadin, L., Chenu, C., Barré, P., 2022. A robust initialization method for accurate soil organic carbon simulations. Biogeosciences 19, 375–387. https://doi.org/10.5194/bg-19-375-2022.
Kaspar, T.C., Singer, J.W., 2015. The use of cover crops to manage soil, in: Soil Management: Building a Stable Base for Agriculture. https://doi.org/10.2136/2011.soilmanagement.c21.
Kassambara, A., 2023. ggpubr: ggplot2 Based Publication Ready Plots.
Kedi, B., Sei, J., Quiquampoix, H., Staunton, S., 2013. Persistence of catalytic activity of fungal phosphatases incubated in tropical soils. Soil Biol. Biochem. 56, 69–74. https://doi.org/10.1016/J.SOILBIO.2012.02.005.
Khan, K.S., Mack, R., Castillo, X., Kaiser, M., Joergensen, R.G., 2016. Microbial biomass, fungal and bacterial residues, and their relationships to the soil organic matter C/N/P/S ratios. Geoderma 271, 115–123. https://doi.org/10.1016/J.GEODERMA.2016.02.019.
Kleber, M., Eusterhues, K., Keiluweit, M., Mikutta, C., Mikutta, R., Nico, P.S., 2015. Mineral-organic associations: formation, properties, and relevance in soil environments. Adv. Agron. 130, 1–140. https://doi.org/10.1016/bs.agron.2014.10.005.
Kleber, M., Sollins, P., Sutton, R., 2007. A conceptual model of organo-mineral interactions in soils: self-assembly of organic molecular fragments into zonal structures on mineral surfaces. Biogeochemistry 85, 9–24. https://doi.org/10.1007/s10533-007-9103-5.
Kohl, L., Laganière, J., Edwards, K.A., Billings, S.A., Morrill, P.L., Van Biesen, G., Ziegler, S.E., 2015. Distinct fungal and bacterial δ13C signatures as potential drivers of increasing δ13C of soil organic matter with depth. Biogeochemistry. https://doi.org/10.1007/s10533-015-0107-2.
Kopittke, P.M., Berhe, A.A., Carrillo, Y., Cavagnaro, T.R., Chen, D., Chen, Q.L., Román Dobarco, M., Dijkstra, F.A., Field, D.J., Grundy, M.J., He, J.Z., Hoyle, F.C., Kögel-Knabner, I., Lam, S.K., Marschner, P., Martinez, C., McBratney, A.B., McDonald-Madden, E., Menzies, N.W., Mosley, L.M., Mueller, C.W., Murphy, D.V., Nielsen, U. N., O'Donnell, A.G., Pendall, E., Pett-Ridge, J., Rumpel, C., Young, I.M., Minasny, B., 2022. Ensuring planetary survival: the centrality of organic carbon in balancing the multifunctional nature of soils. Crit. Rev. Environ. Sci. Technol. https://doi.org/10.1080/10643389.2021.2024484.
Krüger, N., Finn, D.R., Don, A., 2024. Soil depth gradients of organic carbon-13 – a review on drivers and processes. Plant and Soil. https://doi.org/10.1007/s11104-023-06328-5.
Lavallee, J.M., Soong, J.L., Cotrufo, M.F., 2020. Conceptualizing soil organic matter into particulate and mineral-associated forms to address global change in the 21st century. Glob. Chang. Biol. 26, 261–273. https://doi.org/10.1111/gcb.14859.
Lee, J., Hopmans, J.W., Rolston, D.E., Baer, S.G., Six, J., 2009. Determining soil carbon stock changes: simple bulk density corrections fail. Agric. Ecosyst. Environ. 134, 251–256. https://doi.org/10.1016/J.AGEE.2009.07.006.
Lehmann, J., Hansel, C.M., Kaiser, C., Kleber, M., Maher, K., Manzoni, S., Nunan, N., Reichstein, M., Schimel, J.P., Torn, M.S., Wieder, W.R., Kögel-Knabner, I., 2020. Persistence of soil organic carbon caused by functional complexity. Nat. Geosci. 13, 529–534. https://doi.org/10.1038/s41561-020-0612-3.
Lehmann, J., Kleber, M., 2015. The contentious nature of soil organic matter. Nature 528, 60–68. https://doi.org/10.1038/nature16069.
Li, S., Zheng, X., Liu, C., Yao, Z., Zhang, W., Han, S., 2018. Influences of observation method, season, soil depth, land use and management practice on soil dissolvable organic carbon concentrations: a meta-analysis. Sci. Total Environ. 631–632, 105–114. https://doi.org/10.1016/J.SCITOTENV.2018.02.238.
Li, J., Li, S., Zhao, R., Xing, S., Chen, H., Huang, Y., Zhang, L., Li, J., 2025. Soil organic carbon dynamics (2008–2020) across different cultivated land use types in a subtropical region. Geoderma Reg. 40, e00926. https://doi.org/10.1016/J.GEODRS.2025.E00926.
Liang, C., Amelung, W., Lehmann, J., Kästner, M., 2019. Quantitative assessment of microbial necromass contribution to soil organic matter. Glob. Chang. Biol. 25, 3578–3590. https://doi.org/10.1111/gcb.14781.
Liang, C., Schimel, J.P., Jastrow, J.D., 2017. The importance of anabolism in microbial control over soil carbon storage. Nat. Microbiol. 2, 17105. https://doi.org/10.1038/nmicrobiol.2017.105.
Liu, X., Hu, G., He, H., Liang, C., Zhang, W., Bai, Z., Wu, Y., Lin, G., Zhang, X., 2016. Linking microbial immobilization of fertilizer nitrogen to in situ turnover of soil microbial residues in an agro-ecosystem. Agric. Ecosyst. Environ. 229, 40–47. https://doi.org/10.1016/J.AGEE.2016.05.019.
Lorenz, K., Lal, R., 2005. The depth distribution of soil organic carbon in relation to land use and management and the potential of carbon sequestration in subsoil horizons. Adv. Agron. 88, 35–66. https://doi.org/10.1016/S0065-2113(05)88002-2.
Mangiafico, S., 2024. rcompanion: Functions to Support Extension Education Program Evaluation.
Manzoni, S., Cotrufo, M.F., 2024. Mechanisms of soil organic carbon and nitrogen stabilization in mineral-associated organic matter – insights from modeling in phase space. Biogeosciences 21, 4077–4098. https://doi.org/10.5194/bg-21-4077-2024.
Marschner, B., Brodowski, S., Dreves, A., Gleixner, G., Gude, A., Grootes, P.M., Hamer, U., Heim, A., Jandl, G., Ji, R., Kaiser, K., Kalbitz, K., Kramer, C., Leinweber, P., Rethemeyer, J., Schäffer, A., Schmidt, M.W.I., Schwark, L., Wiesenberg, G.L.B., 2008. How relevant is recalcitrance for the stabilization of organic matter in soils? J. Plant Nutr. Soil Sci. https://doi.org/10.1002/jpln.200700049.
Mary, B., Clivot, H., Blaszczyk, N., Labreuche, J., Ferchaud, F., 2020. Soil carbon storage and mineralization rates are affected by carbon inputs rather than physical disturbance: evidence from a 47-year tillage experiment. Agric. Ecosyst. Environ. 299, 106972. https://doi.org/10.1016/j.agee.2020.106972.
Mathieu, J.A., Hatté, C., Balesdent, J., Parent, É., 2015. Deep soil carbon dynamics are driven more by soil type than by climate: a worldwide meta-analysis of radiocarbon profiles. Glob. Chang. Biol. 21, 4278–4292. https://doi.org/10.1111/gcb.13012.
Mattila, T.J., Hagelberg, E., Söderlund, S., Joona, J., 2022. How farmers approach soil carbon sequestration? Lessons learned from 105 carbon-farming plans. Soil Tillage Res. 215. https://doi.org/10.1016/j.still.2021.105204.
Menichetti, L., Ekblad, A., Kätterer, T., 2015. Contribution of roots and amendments to soil carbon accumulation within the soil profile in a long-term field experiment in Sweden. Agric. Ecosyst. Environ. 200, 79–87. https://doi.org/10.1016/J.AGEE.2014.11.003.
Meyer, N., Sietiö, O.M., Adamczyk, S., Ambus, P., Biasi, C., Glaser, B., Kalu, S., Martin, A., Mganga, K.Z., Olin, M., Seppänen, A., Shrestha, R., Karhu, K., 2023. Fate and stabilization of labile carbon in a sandy boreal forest soil – a question of nitrogen availability? Appl. Soil Ecol. 191. https://doi.org/10.1016/j.apsoil.2023.105052.
Moragues-Saitua, L., Merino-Martín, L., Stokes, A., Staunton, S., 2019. Towards meaningful quantification of glomalin-related soil protein (GRSP) taking account of interference in the Coomassie Blue (Bradford) assay. Eur. J. Soil Sci. 70, 727–735. https://doi.org/10.1111/ejss.12698.
Nautiyal, P., Rajput, R., Pandey, D., Arunachalam, K., Arunachalam, A., 2019. Role of glomalin in soil carbon storage and its variation across land uses in temperate Himalayan regime. Biocatal. Agric. Biotechnol. 21, 101311. https://doi.org/10.1016/J.BCAB.2019.101311.
Ni, X., Liao, S., Tan, S., Wang, D., Peng, Y., Yue, K., Wu, F., Yang, Y., 2020. A quantitative assessment of amino sugars in soil profiles. Soil Biol. Biochem. 143. https://doi.org/10.1016/j.soilbio.2020.107762.
Oehl, F., Sieverding, E., Ineichen, K., Mäder, P., Boller, T., Wiemken, A., 2003. Impact of land use intensity on the species diversity of arbuscular mycorrhizal fungi in agroecosystems of Central Europe. Appl. Environ. Microbiol. 69. https://doi.org/10.1128/AEM.69.5.2816-2824.2003.
Ogle, D.H., Doll, J.C., Powell Wheeler, A., Dinno, A., 2023. FSA: Simple Fisheries Stock Assessment Methods.

Palonen, V., 2015. A portable molecular-sieve-based CO2 sampling system for radiocarbon measurements. Rev. Sci. Instrum. 86, 125101. https://doi.org/10.1063/1.4936291.
Palonen, V., Tikkanen, P., 2015. A novel upgrade to Helsinki AMS: fast switching of isotopes with electrostatic deflectors. Nucl. Instrum. Methods Phys. Res. B 361, 263–266. https://doi.org/10.1016/J.NIMB.2015.04.053.
Palosuo, T., Heikkinen, J., Regina, K., 2015. Method for estimating soil carbon stock changes in Finnish mineral cropland and grassland soils. Carbon Manag. 6, 207–220. https://doi.org/10.1080/17583004.2015.1131383.
Pellerin, S., Bamière, L., Launay, C., Martin, R., Schiavo, M., Angers, D., Augusto, L., Balesdent, J., Basile-Doelsch, I., Bellassen, V., Cardinael, R., Cécillon, L., Ceschia, E., Chenu, C., Constantin, J., Darroussin, J., Delacote, P., Delame, N., Gastal, F., Gilbert, D., Graux, A.-I., Guenet, B., Houot, S., Klumpp, K., Letort, E., Litrico, I., Martin, M., Menasseri, S., Mézière, D., Morvan, T., Mosnier, C., Roger-Estrade, J., Saint-André, L., Sierra, J., Thérond, O., Viaud, V., Grateau, R., Le Perchec, S., Savini, I., Réchauchère, O., 2020. Stocker du carbone dans les sols français, Quel potentiel au regard de l'objectif 4 pour 1000 et à quel coût ? Rapport scientifique de l'étude. INRA (France) 540, 540.
Plante, A.F., Beaupré, S.R., Roberts, M.L., Baisden, T., 2013. Distribution of radiocarbon ages in soil organic matter by thermal fractionation. Radiocarbon 55, 1077–1083. https://doi.org/10.1017/s0033822200058215.
Poeplau, C., Begill, N., Liang, Z., Schiedung, M., 2023. Root litter quality drives the dynamic of native mineral-associated organic carbon in a temperate agricultural soil. Plant and Soil 491, 439–456. https://doi.org/10.1007/s11104-023-06127-y.
Poeplau, C., Don, A., 2013. Sensitivity of soil organic carbon stocks and fractions to different land-use changes across Europe. Geoderma 192, 189–201. https://doi.org/10.1016/j.geoderma.2012.08.003.
Poeplau, C., Don, A., Vesterdal, L., Leifeld, J., Van Wesemael, B., Schumacher, J., Gensior, A., 2011. Temporal dynamics of soil organic carbon after land-use change in the temperate zone - carbon response functions as a model approach. Glob. Chang. Biol. 17, 2415–2427. https://doi.org/10.1111/j.1365-2486.2011.02408.x.
Poirier, N., Sohi, S.P., Gaunt, J.L., Mahieu, N., Randall, E.W., Powlson, D.S., Evershed, R. P., 2005. The chemical composition of measurable soil organic matter pools. Org Geochem. 36, 1174–1189. https://doi.org/10.1016/J.ORGGEOCHEM.2005.03.005.
R Core Team, 2023. R: A Language and Environment for Statistical Computing.
Rasse, D.P., Mulder, J., Moni, C., Chenu, C., 2006. Carbon turnover kinetics with depth in a French loamy soil. Soil Sci. Soc. Am. J. 70, 2097–2105. https://doi.org/10.2136/sssaj2006.0056.
Reimer, P.J., Austin, W.E.N., Bard, E., Bayliss, A., Blackwell, P.G., Bronk Ramsey, C., Butzin, M., Cheng, H., Edwards, R.L., Friedrich, M., Grootes, P.M., Guilderson, T.P., Hajdas, I., Heaton, T.J., Hogg, A.G., Hughen, K.A., Kromer, B., Manning, S.W., Muscheler, R., Palmer, J.G., Pearson, C., van der Plicht, J., Reimer, R.W., Richards, D.A., Scott, E.M., Southon, J.R., Turney, C.S.M., Wacker, L., Adolphi, F., Büntgen, U., Capano, M., Fahrni, S.M., Fogtmann-Schulz, A., Friedrich, R., Köhler, P., Kudsk, S., Miyake, F., Olsen, J., Reinig, F., Sakamoto, M., Sookdeo, A., Talamo, S., 2020. The IntCal20 Northern Hemisphere Radiocarbon Age Calibration Curve (0–55 cal kBP). Radiocarbon 62, 725–757. https://doi.org/DOI: 10.1017/RDC.2020.41.
Rillig, M.C., 2004. Arbuscular mycorrhizae, glomalin, and soil aggregation. Can. J. Soil Sci. 84, 355–363. https://doi.org/10.4141/S04-003.
Rillig, M.C., Ramsey, P.W., Morris, S., Paul, E.A., 2003. Glomalin, an arbuscular-mycorrhizal fungal soil protein, responds to land-use change. Plant and Soil.
Rillig, M.C., Wright, S.F., Nichols, K.A., Schmidt, W.F., Torn, M.S., 2001. Large contribution of arbuscular mycorrhizal fungi to soil carbon pools in tropical forest soils. Plant and Soil 233. https://doi.org/10.1023/A:1010364221169.
Salminen, R., Kukkonen, M., Paukola, T., Toellikkoe, S., 1997. Chemical composition of clays in southwestern Finland. Special Paper-Geological Survey of Finland 117–126.
Salonen, A.R., Soinne, H., Creamer, R., Lemola, R., Ruoho, N., Uhlgren, O., de Goede, R., Heinonsalo, J., 2023. Assessing the effect of arable management practices on carbon storage and fractions after 24 years in boreal conditions of Finland. Geoderma Reg. 34. https://doi.org/10.1016/j.geodrs.2023.e00678.
Sanderman, J., Grandy, A.S., 2020. Ramped thermal analysis for isolating biologically meaningful soil organic matter fractions with distinct residence times. Soil 6, 131–144. https://doi.org/10.5194/soil-6-131-2020.
Sanderman, J., Hengl, T., Fiske, G.J., 2017. Soil carbon debt of 12,000 years of human land use. PNAS 115, 9575–9580. https://doi.org/10.1073/pnas.1800925115.
Schiedung, M., Barré, P., Peoplau, C., 2025. Separating fast from slow cycling soil organic carbon – a multi-method comparison on land use change sites. Geoderma 453. https://doi.org/10.1016/j.geoderma.2024.117154.
Schmidt, M.W.I., Torn, M.S., Abiven, S., Dittmar, T., Guggenberger, G., Janssens, I.A., Kleber, M., Kögel-Knabner, I., Lehmann, J., Manning, D.A.C., Nannipieri, P., Rasse, D.P., Weiner, S., Trumbore, S.E., 2011. Persistence of soil organic matter as an ecosystem property. Nature. https://doi.org/10.1038/nature10386.
Schneider, F., Amelung, W., Don, A., 2021. Origin of carbon in agricultural soil profiles deduced from depth gradients of C:N ratios, carbon fractions, δ13C and δ15N values. Plant and Soil 460, 123–148. https://doi.org/10.1007/s11104-020-04769-w.
Schweizer, S.A., 2022. Perspectives from the Fritz-Scheffer Awardee 2021: soil organic matter storage and functions determined by patchy and piled-up arrangements at the microscale. J. Plant Nutr. Soil Sci. 185, 694–706. https://doi.org/10.1002/jpln.202200217.
Shahzad, T., Rashid, M.I., Maire, V., Barot, S., Perveen, N., Alvarez, G., Mougin, C., Fontaine, S., 2018. Root penetration in deep soil layers stimulates mineralization of millennia-old organic carbon. Soil Biol. Biochem. 124, 150–160. https://doi.org/10.1016/J.SOILBIO.2018.06.010.
Shi, Z., Allison, S.D., He, Y., Levine, P.A., Hoyt, A.M., Beem-Miller, J., Zhu, Q., Wieder, W.R., Trumbore, S., Randerson, J.T., 2020. The age distribution of global soil carbon inferred from radiocarbon measurements. Nat. Geosci. 13, 555–559. https://doi.org/10.1038/s41561-020-0596-z.
Sierra, C.A., Müller, M., Metzler, H., Manzoni, S., Trumbore, S.E., 2017. The muddle of ages, turnover, transit, and residence times in the carbon cycle. Glob. Chang. Biol. 23, 1763–1773. https://doi.org/10.1111/gcb.13556.
Six, J., Jastrow, J., 2002. Organic Matter Turnover, in: Lal, R. (Ed.), Encyclopedia of Soil Science. Marcel Dekker, pp. 936–942. https://doi.org/10.1201/noe0849338304.ch252.
Skadell, L.E., Schneider, F., Gocke, M.I., Guigue, J., Amelung, W., Bauke, S.L., Hobley, E. U., Barkusky, D., Honermeier, B., Kögel-Knabner, I., Schmidhalter, U., Schweitzer, K., Seidel, S.J., Siebert, S., Sommer, M., Vaziritabar, Y., Don, A., 2023. Twenty percent of agricultural management effects on organic carbon stocks occur in subsoils – results of ten long-term experiments. Agric. Ecosyst. Environ. 356, 108619. https://doi.org/10.1016/J.AGEE.2023.108619.
Smith, P., 2008. Land use change and soil organic carbon dynamics. Nutr. Cycl. Agroecosyst. 81, 169–178. https://doi.org/10.1007/s10705-007-9138-y.
Smith, P., Chapman, S.J., Scott, W.A., Black, H.I.J., Wattenbach, M., Milne, R., Campbell, C.D., Lilly, A., Ostle, N., Levy, P.E., Lumsdon, D.G., Millard, P., Towers, W., Zaehle, S., Smith, J.U., 2007. Climate change cannot be entirely responsible for soil carbon loss observed in England and Wales, 1978-2003. Glob. Chang. Biol. 13, 2605–2609. https://doi.org/10.1111/j.1365-2486.2007.01458.x.
Sokol, N.W., Whalen, E.D., Jilling, A., Kallenbach, C., Pett-Ridge, J., Georgiou, K., 2022. Global distribution, formation and fate of mineral-associated soil organic matter under a changing climate: a trait-based perspective. Funct. Ecol. https://doi.org/10.1111/1365-2435.14040.
Soucémarianadin, L., Cécillon, L., Guenet, B., Chenu, C., Baudin, F., Nicolas, M., Girardin, C., Barré, P., 2018. Environmental factors controlling soil organic carbon stability in French forest soils environmental factors controlling soil organic carbon stability in French forest soils. Plant and Soil 426–427. https://doi.org/10.1007/s11104-018-3613-xï.
Staunton, S., Saby, N.P.A., Arrouays, D., Quiquampoix, H., 2020. Can soil properties and land use explain glomalin-related soil protein (GRSP) accumulation? A Nationwide Survey in France. Catena (Amst) 193, 104620. https://doi.org/10.1016/J.CATENA.2020.104620.
Stockmann, U., Adams, M.A., Crawford, J.W., Field, D.J., Henakaarchchi, N., Jenkins, M., Minasny, B., McBratney, A.B., Courcelles, V. de R. de, Singh, K., Wheeler, I., Abbott, L., Angers, D.A., Baldock, J., Bird, M., Brookes, P.C., Chenu, C., Jastrow, J. D., Lal, R., Lehmann, J., O'Donnell, A.G., Parton, W.J., Whitehead, D., Zimmermann, M., 2013. The knowns, known unknowns and unknowns of sequestration of soil organic carbon. Agric. Ecosyst. Environ. https://doi.org/10.1016/j.agee.2012.10.001.
Stoner, S., Trumbore, S.E., González-Pérez, J.A., Schrumpf, M., Sierra, C.A., Hoyt, A.M., Chadwick, O., Doetterl, S., 2023. Relating mineral-organic matter stabilization mechanisms to carbon quality and age distributions using ramped thermal analysis. Philos. Trans. R. Soc. A Math. Phys. Eng. Sci. 381. https://doi.org/10.1098/rsta.2023.0139.
Struecker, J., Joergensen, R.G., 2015. Microorganisms and their substrate utilization patterns in topsoil and subsoil layers of two silt loams, differing in soil organic C accumulation due to colluvial processes. Soil Biol. Biochem. 91, 310–317. https://doi.org/10.1016/J.SOILBIO.2015.09.011.
Styc, Q., Minasny, B., Jang, H.J., McBratney, A., 2025. Modelling soil organic carbon dynamics at the continental extent using pedogenon mapping. Eur. J. Soil Sci. 76, e70070. https://doi.org/10.1111/ejss.70070.
Tautges, N.E., Chiartas, J.L., Gaudin, A.C.M., O'Geen, A.T., Herrera, I., Scow, K.M., 2019. Deep soil inventories reveal that impacts of cover crops and compost on soil carbon sequestration differ in surface and subsurface soils. Glob. Chang. Biol. 25. https://doi.org/10.1111/gcb.14762.
Tikkanen, P., Palonen, V., Jungner, H., Keinonen, J., 2004. AMS facility at the University of Helsinki. Nucl. Instrum. Methods Phys. Res. B 223–224, 35–39. https://doi.org/10.1016/J.NIMB.2004.04.011.
Torn, M.S., Swanston, C.W., Castanha, C., Trumbore, S.E., 2009. Storage and Turnover of Organic Matter in Soil, in: Biophysico-Chemical Processes Involving Natural Nonliving Organic Matter in Environmental Systems. John Wiley & Sons, Ltd, pp. 219–272. https://doi.org/https://doi.org/10.1002/9780470494950.ch6.
Torn, M.S., Trumbore, S.E., Chadwick, O.A., Vitousek, P.M., Hendricks, D.M., 1997. Mineral control of soil organic carbon storage and turnover content were measured by horizon down to the depth at which. Nature 389, 3601–3603.
Trumbore, S., 2009. Radiocarbon and soil carbon dynamics. Annu. Rev. Earth Planet. Sci. https://doi.org/10.1146/annurev.earth.36.031207.124300.
Trumbore, S., 2000. Age of soil organic matter and soil respiration: radiocarbon constraints on belowground C dynamics. Ecol. Appl. 10, 399–411. https://doi.org/10.1890/1051-0761(2000)010[0399:AOSOMA]2.0.CO;2.
Trumbore, S., 1997. Potential responses of soil organic carbon to global environmental change. PNAS 94, 8284–8291.
Trumbore, S.E., Vogel, J.S., Southon, J.R., 1989. AMS 14C Measurements of fractionated soil organic matter: an approach to deciphering the soil carbon cycle. Radiocarbon 31, 644–654. https://doi.org/DOI: 10.1017/S0033822200012248.
Uusitalo, J., Arppe, L., Helama, S., Mizohata, K., Mielikäinen, K., Mäkinen, H., Nöjd, P., Timonen, M., Oinonen, M., 2022. From lakes to ratios: 14C measurement process of the Finnish tree-ring research consortium. Nucl. Instrum. Methods Phys. Res. B 519, 37–45. https://doi.org/10.1016/J.NIMB.2022.03.013.
Vogel, C., Mueller, C.W., Höschen, C., Buegger, F., Heister, K., Schulz, S., Schloter, M., Kögel-Knabner, I., 2014. Submicron structures provide preferential spots for carbon and nitrogen sequestration in soils. Nat. Commun. 5, 2947. https://doi.org/10.1038/ncomms3947.

von Lützow, M., Kögel-Knabner, I., Ekschmitt, K., Flessa, H., Guggenberger, G., Matzner, E., Marschner, B., 2007. SOM fractionation methods: relevance to functional pools and to stabilization mechanisms. Soil Biol. Biochem. 39, 2183–2207. https://doi.org/10.1016/j.soilbio.2007.03.007.

von Lützow, M., Kögel-Knabner, I., Ekschmitt, K., Matzner, E., Guggenberger, G., Marschner, B., Flessa, H., 2006. Stabilization of organic matter in temperate soils: mechanisms and their relevance under different soil conditions - a review. Eur. J. Soil Sci. 57, 426–445. https://doi.org/10.1111/j.1365-2389.2006.00809.x.

Wang, B., An, S., Liang, C., Liu, Y., Kuzyakov, Y., 2021. Microbial necromass as the source of soil organic carbon in global ecosystems. Soil Biol. Biochem. 162, 108422. https://doi.org/10.1016/J.SOILBIO.2021.108422.

Wang, W., Zhong, Z., Wang, Q., Wang, H., Fu, Y., He, X., 2017. Glomalin contributed more to carbon, nutrients in deeper soils, and differently associated with climates and soil properties in vertical profiles. Sci. Rep. 7, 13003. https://doi.org/10.1038/s41598-017-12731-7.

Wendt, J.W., Hauser, S., 2013. An equivalent soil mass procedure for monitoring soil organic carbon in multiple soil layers. Eur. J. Soil Sci. 64, 58–65. https://doi.org/10.1111/ejss.12002.

Wickham, H., 2016. ggplot2: Elegant Graphics for Data Analysis. Springer-Verlag, New York.

Wickham, H., 2007. Reshaping data with the reshape package. J. Stat. Softw. 21, 1–20. https://doi.org/10.18637/jss.v021.i12.

Wickham, H., François, R., Lionel Henry, Müller, K., Vaughan, D., 2023. dplyr: A Grammar of Data Manipulation.

Woignier, T., Etcheverria, P., Borie, F., Quiquampoix, H., Staunton, S., 2014. Role of allophanes in the accumulation of glomalin-related soil protein in tropical soils (Martinique, French West Indies). Eur. J. Soil Sci. 65, 531–538. https://doi.org/10.1111/ejss.12151.

Wright, S.F., Upadhyaya, A., 1996. Extraction of an abundant and unusual protein from soil and comparison with hyphal protein of arbuscular mycorrhizal fungi. Soil Sci. 161.

Yang, Y., Dou, Y., Wang, B., Wang, Y., Liang, C., An, S., Soromotin, A., Kuzyakov, Y., 2022. Increasing contribution of microbial residues to soil organic carbon in grassland restoration chronosequence. Soil Biol. Biochem. 170, 108688. https://doi.org/10.1016/J.SOILBIO.2022.108688.

Yli-Halla, M., 2000. Suomalaisia maaprofiileja : agricultural soil profiles in finland and their classification. publications of agricultural research centre of Finland. Serie A 78. A. Agricultural Research Centre of Finland, Jokioinen.

Zhang, X., Amelung, W., 1996. Gas chromatographic determination of muramic acid, glucosamine, mannosamine, and galactosamine in soils. Soil Biol. Biochem. 28, 1201–1206. https://doi.org/10.1016/0038-0717(96)00117-4.

Zhao, Y., Biswas, A., Liu, M., Han, X., Lu, X., Chen, X., Hao, X., Zou, W., 2025. Land use effects on soil carbon retention through glomalin-mediated aggregation. Geoderma 456, 117252. https://doi.org/10.1016/J.GEODERMA.2025.117252.